



Wind Resource Assessment of Gujarat (India)

C. Draxl, A. Purkayastha, and Z. Parker

**NREL is a national laboratory of the U.S. Department of Energy
Office of Energy Efficiency & Renewable Energy
Operated by the Alliance for Sustainable Energy, LLC**

This report is available at no cost from the National Renewable Energy Laboratory (NREL) at www.nrel.gov/publications.

Technical Report
NREL/TP-5000-61741
July 2014

Contract No. DE-AC36-08GO28308

Wind Resource Assessment of Gujarat (India)

C. Draxl, A. Purkayastha, and Z. Parker

Prepared under Task No. IGIN.1401

**NREL is a national laboratory of the U.S. Department of Energy
Office of Energy Efficiency & Renewable Energy
Operated by the Alliance for Sustainable Energy, LLC**

This report is available at no cost from the National Renewable Energy
Laboratory (NREL) at www.nrel.gov/publications.

NOTICE

This report was prepared as an account of work sponsored by an agency of the United States government. Neither the United States government nor any agency thereof, nor any of their employees, makes any warranty, express or implied, or assumes any legal liability or responsibility for the accuracy, completeness, or usefulness of any information, apparatus, product, or process disclosed, or represents that its use would not infringe privately owned rights. Reference herein to any specific commercial product, process, or service by trade name, trademark, manufacturer, or otherwise does not necessarily constitute or imply its endorsement, recommendation, or favoring by the United States government or any agency thereof. The views and opinions of authors expressed herein do not necessarily state or reflect those of the United States government or any agency thereof.

This report is available at no cost from the National Renewable Energy Laboratory (NREL) at www.nrel.gov/publications.

Available electronically at <http://www.osti.gov/scitech>

Available for a processing fee to U.S. Department of Energy and its contractors, in paper, from:

U.S. Department of Energy
Office of Scientific and Technical Information
P.O. Box 62
Oak Ridge, TN 37831-0062
phone: 865.576.8401
fax: 865.576.5728
email: <mailto:reports@adonis.osti.gov>

Available for sale to the public, in paper, from:

U.S. Department of Commerce
National Technical Information Service
5285 Port Royal Road
Springfield, VA 22161
phone: 800.553.6847
fax: 703.605.6900
email: orders@ntis.fedworld.gov
online ordering: <http://www.ntis.gov/help/ordermethods.aspx>

Acknowledgments

The authors would like to extend sincere gratitude to the Centre for Wind Energy Technology, India, for providing wind data from ground measurement stations in Gujarat that we used to validate the modeled data in this analysis, especially to Dr. Gomathinayagam and Mr. Boopathi. We would also like to thank Jason Knievel of the National Center for Atmospheric Research (NCAR) and Andrew Clifton of the National Renewable Energy Laboratory (NREL) for their thoughtful reviews and comments, Julie Lundquist of NREL for her guidance at the beginning of the study, Sarah Booth of NREL for providing valuable input and comments during the editing and production process, and Jennifer Melius of NREL for the data visualization efforts. The wind resource and forecasting simulations were performed on NREL's high-performance computing system Peregrine. Any errors or omissions are solely the responsibility of the authors.

This analysis was funded by the U.S. Department of Energy's Office of Energy Efficiency & Renewable Energy and developed in coordination with India's Ministry of New and Renewable Energy under the U.S.-India Energy Dialogue's New Technology and Renewable Energy Working Group.

Nomenclature or List of Acronyms

ABL	Above ground level
CWET	Centre for Wind Energy Technology
CRMSE	Centered root-mean-squared error
ECMWF	European Centre for Medium-Range Weather Forecasts
GFS	Global Forecast System
GWh	Gigawatt-hours
IRENA	International Renewable Energy Agency
MAE	Mean absolute error
NCAR	National Center for Atmospheric Research
NCEP	National Centers for Environmental Prediction
NREL	National Renewable Energy Laboratory
NWP	Numerical weather prediction
PBL	Planetary boundary layer
QNSE	Quasi-normal scale elimination
RMSE	Root-mean-squared error
SST	Sea surface temperature
USGS	United States Geological Service
WDE	Wind distribution error
WRF	Weather Research and Forecasting Model
YSU	Yonsei University

Executive Summary

India is one of the largest wind energy markets in the world. The first Indian state to install a wind power project was Gujarat in 1986. In February 2013, the installed wind capacity in Gujarat was 3,093 MW. Multiple contradicting wind resource assessments exist for India. Owing to the uncertainty around these existing wind energy assessments, this analysis uses the Weather Research and Forecasting (WRF) model to simulate the wind at current hub heights for one year to provide more precise estimates of wind resources in Gujarat. The WRF model allows for accurate simulations of winds near the surface and at heights important for wind energy purposes. While previous resource assessments published wind power density, we focus on average wind speeds, which can be converted to wind power densities by the user with methods of their choice.

Prior to the one-year simulations, we carried out a sensitivity study using two weeks each in January, April, and August 2011. This sensitivity study covers the main seasons, and served to find the optimal boundary conditions, grid spacings, and physics settings in the model that give best results for Gujarat. The sensitivity study showed that a finer horizontal resolution results in better resource estimates, but that the increase in accuracy between a grid spacing of 3.3 km and 1.1 km might not be worth the additional computational expense.

We compared our simulations of both the sensitivity study and the year-long simulations to measurements at five locations throughout the country. We validated the model using traditional error metrics such as root-mean-squared error (RMSE), mean absolute error (MAE), and bias; but also against rank correlation, CRMSE, normalized RMSE, and the wind distribution error (WDE). Annual and diurnal cycles, wind roses, and histograms shed further light onto the behavior of the WRF model. Validation results showed a very good agreement of modeled to observed winds. A positive bias was found, leading to an estimated overprediction of less than 0.8 m/s for the annual average. These and the other results presented in this report give us confidence in an accurate wind resource assessment.

The wind resource estimates in this study show regions with average annual wind speeds of more than 8 m/s. These areas are concentrated in the Gulf of Kutch and on the south coast of the peninsula. Previous literature found that the highest wind energy potentials are concentrated in the northwestern part of the state, north of the Gulf of Kutch. In our analysis, the yearly average for 2011 shows the highest potential at the same location but also shows a similarly high potential along the south coast of the peninsula (offshore and on the coast between Sarakhadi Gam and Gadhula). Likewise, the International Renewable Energy Agency identified the highest wind speeds to be in the Gulf of Kutch and the southern tip of the peninsula. They also identified the Gulf of Khambhat to have average wind speeds of 9 m/s, which is higher than our estimate.

Conforming with the usual seasonal cycle that can be expected in India and with validation results at five measurement sites, the wind speed is highest in the summer from May to August, with maximum average wind speeds of higher than 10 m/s, especially along the coast lines during these months. The wind speeds are lowest in October and November with average wind speeds not exceeding 7 m/s at coastal sites.

Table of Contents

List of Figures	5
List of Tables	7
1 Introduction	8
2 Data and Methods	9
2.1 Mesoscale Model Simulations	9
2.2 Observations	11
2.3 Climate in Gujarat	11
2.4 Validation Methods	12
3 Sensitivity Study	12
3.1 Model Setup	13
3.2 Results from Sensitivity Study and Implications	13
4 Gujarat’s Wind Resource	18
4.1 Results	18
4.2 Wind Resource Validation	22
4.2.1 Histograms	22
4.2.2 Error Metrics	22
4.2.3 Impact of Temporal Resolution	24
4.2.4 Diurnal Cycles	24
4.2.5 Wind Roses	25
4.2.6 Annual Cycle	25
4.3 Comparisons of Simulations with Existing Wind Resource Estimates for Gujarat	29
5 Summary and Conclusion	30
References	33
Appendix	36

List of Figures

Figure 1. WRF simulation domains. Terrain elevation from domain 1 (33.3 km grid) is shown in domains 1–3, and from domain 4 (1.1 km grid) in domain 4. The crosses denote observation locations of the 5 measurement sites: purple - Balava, red - Jikiali, yellow - Virewa, blue - Sarva, brown - Jegawa.....	10
Figure 2: Histograms of wind speed for all the experiments and five locations, as indicated by the legend and title, respectively. Modeled wind speeds are at 80 m, observed at 50 m.....	15
Figure 3: Wind roses for modeled wind speeds in meters per second at 112 m and observed at 50 m (bottom right) for Balava.....	16
Figure 4: Annual average wind speeds at 80 m.....	19
Figure 5: Annual average wind speeds at 112 m.....	20
Figure 6: Average wind speeds for every month during 2011.....	21
Figure 7: Histograms of observed (dashed lines) and simulated (solid lines) wind speed at 50 m at the five measurement sites as indicated in the title of each panel.....	23
Figure 8: Average diurnal cycle of wind speeds at different heights for Jegawa as indicated in the panel titles. Simulated wind speeds are in blue, observed in green.....	26
Figure 9: Wind roses for observed wind speeds in meters per second at 50 m (left column) and simulated wind speeds at 80 m (right column) for the five measurement sites.....	27
Figure 10: Sarva’s annual cycle of simulated wind speed at 50 m, 80 m, and 112 m, and observed wind speeds at 50 m (panel a), wind speed bias for winds at 50 m (simulated minus observed; panel b), and normalized RMSE of wind speeds at 50 m (panel c).....	28
Figure 11: Wind power density at 50 m (left) and 80 m (right). From CWET (CWET 2014).....	29
Figure 12: Screenshot of wind speed estimates from Irena (http://irena.masdar.ac.ae/?map=178 , accessed May 2014).....	30
Figure 13: Histograms for each month in 2011 of 50 m observed (dashed lines) and simulated (solid lines) wind speeds for Balava.....	36
Figure 14: Histograms for each month in 2011 of 50 m observed (dashed lines) and simulated (solid lines) wind speeds for Jegawa.....	37
Figure 15: Histograms for each month in 2011 of 50 m observed (dashed lines) and simulated (solid lines) wind speeds for Virewa.....	38
Figure 16: Histograms for each month in 2011 of 50 m observed (dashed lines) and simulated (solid lines) wind speeds for Sarva.....	39
Figure 17: Histograms for each month in 2011 of 50 m observed (dashed lines) and simulated (solid lines) wind speeds for Jikiali.....	40
Figure 18: Average diurnal cycle of wind speeds at different heights as indicated in the panel titles for Virewa. Simulated wind speeds are in blue, observed in green.....	41
Figure 19: Average diurnal cycle of wind speeds at different heights as indicated in the panel titles for Sarva. Simulated wind speeds are in blue, observed in green.....	42
Figure 20: Average diurnal cycle of wind speeds at different heights as indicated in the panel titles for Jikiali. Simulated wind speeds are in blue, observed in green.....	43
Figure 21: Average diurnal cycle of wind speeds at different heights as indicated in the panel titles for Balava. Simulated wind speeds are in blue, observed in green.....	44
Figure 22: Wind roses for every month of the year 2011 as modeled by WRF for 80 m for Balava.....	45

Figure 23: Wind roses of measured wind speed and direction for every month of the year 2011 for 50 m for Balava.	46
Figure 24: Annual cycle of simulated wind speed at 50 m, 80 m, and 112 m, and observed wind speeds at 50 m (panel a), wind speed bias for winds at 50 m (simulated minus observed; panel b), and normalized RMSE of wind speeds at 50 m (panel c) for Jikiali.	47
Figure 25: Annual cycle of simulated wind speed at 50 m, 80 m, and 112 m, and observed wind speeds at 50 m (panel a), wind speed bias for winds at 50 m (simulated minus observed; panel b), and normalized RMSE of wind speeds at 50 m (panel c) for Balava.....	48
Figure 26: Annual cycle of simulated wind speed at 50 m, 80 m, and 112 m, and observed wind speeds at 50 m (panel a), wind speed bias for winds at 50 m (simulated minus observed; panel b), and normalized RMSE of wind speeds at 50 m (panel c) for Jegawa.	49
Figure 27: Annual cycle of simulated wind speed at 50 m, 80 m, and 112 m, and observed wind speeds at 50 m (panel a), wind speed bias for winds at 50 m (simulated minus observed; panel b), and normalized RMSE of wind speeds at 50 m (panel c) for Virewa.....	50
Figure 28: Diurnal cycle of (a) bias and (b) RMSE of wind speeds at 50 m for the winter months (January, February, March, October, November, December) for Jegawa.	51
Figure 29: Diurnal cycle of (a) bias and (b) RMSE of wind speeds at 50 m for the winter months (January, February, March, October, November, December) for Virewa.....	51
Figure30: Diurnal cycle of (a) bias and (b) RMSE of wind speeds at 50 m for the winter months (January, February, March, October, November, December) for Sarva.	52
Figure 31: Diurnal cycle of (a) bias and (b) RMSE of wind speeds at 50 m for the winter months (January, February, March, October, November, December) for Jikiali.	52
Figure 32: Diurnal cycle of (a) bias and (b) RMSE of wind speeds at 50 m for the winter months (January, February, March, October, November, December) for Balava.....	53
Figure 33: Diurnal cycle of (a) bias and (b) RMSE of wind speeds at 50 m for the summer months (April, May, June, July, August, September) for Jegawa.	53
Figure 34: Diurnal cycle of (a) bias and (b) RMSE of wind speeds at 50 m for the summer months (April, May, June, July, August, September) for Virewa.....	54
Figure 35: Diurnal cycle of (a) bias and (b) RMSE of wind speeds at 50 m for the summer months (April, May, June, July, August, September) for Sarva.	54
Figure 36: Diurnal cycle of (a) bias and (b) RMSE of wind speeds at 50 m for the summer months (April, May, June, July, August, September) for Jikiali.	55
Figure 37: Diurnal cycle of (a) bias and (b) RMSE of wind speeds at 50 m for the summer months (April, May, June, July, August, September) for Balava.....	55

List of Tables

Table 1: Observation Locations	11
Table 2: Error Metrics Used in the Analysis	13
Table 3. Experiments for Sensitivity Study	14
Table 4. Error Metrics for the Sensitivity Study for 50 m Wind Speeds Averaged for All the Sites.....	17
Table 5: Error Metrics for the Sensitivity Study for 112 m Wind Speeds Averaged for All the Sites.....	17
Table 6. Error Metrics for 2011 for 10-min Model Output for 50 m in meters per second.....	24
Table 7. Error Metrics for 2011 for Hourly Model Output for 50 m in Meters per Second. (A more detailed breakdown of RMSE and bias into diurnal cycles per month for all the 5 stations is in the appendix, Figure 28 through Figure 37).	24

1 Introduction

India is one of the largest wind energy markets in the world. Renewable energy sources represent 12.2% of India's installed capacity, with 70% of this contribution coming from wind energy (International Renewable Energy Agency, 2014). The first Indian state to install a wind power project was Gujarat in 1986 (Centre for Wind Energy Technology [CWET], 2014). In February 2013, the installed wind capacity in Gujarat was 3,093 MW. Tamil Nadu, in southeast India, is the only state with more installed wind capacity than Gujarat. The installed capacity in Gujarat is expected to increase as future projects are planned, including an offshore wind farm in the Gulf of Khambhat in the southeastern region of the state (Patel et al, 2011). Accurate wind resource estimates are crucial to support the development of wind energy in Gujarat.

There have been multiple wind resource assessments conducted for India. The first surveys, which used data from wind monitoring stations with towers that were 20–25 meters tall, showed promising wind resources in Gujarat (Mani and Mooley, 1983); however, that height is too low for current wind turbines. Additional wind resource assessments or mention of wind power for India can be found in publications by Jagadeesh (1985), Jagadeesh (1987), Rao (1986), Amin (1999), Bakshi (2002), Mooley (1983), and Jaswal and Koppar (2013). The wind resource estimates in India varied depending on the methodology, data, and hub heights used in these reports (Phadke et al, 2011). To address this variation, Phadke et al (2011) analyzed wind resource data across the country. They conducted an extended reassessment study, estimating land-based wind energy potential for 80 m, 100 m, and 120 m. Phadke et al conclude that high quality wind energy sites have more than five times the current official estimate, and 30 times that of the official Indian estimate published in the 2010 Wind Energy Atlas (CWET, 2010). The authors theorize that the most likely reason for the discrepancies between these estimates is the difference in assumed land availability.

Due to the uncertainty around existing wind energy assessments in India, this analysis uses the Weather Research and Forecasting (WRF) model to simulate the wind at current hub heights to provide more precise estimates of wind resources in Gujarat. The wind resource estimates are limited to wind speeds and direction. The WRF model is a community numerical weather prediction (NWP) model maintained by the National Center for Atmospheric Research (NCAR) in the United States, and has been successfully applied to wind energy related studies and wind resource assessments (e.g., Draxl et al, 2012; Draxl et al, 2013; Storm and Basu, 2010; Phadke et al, 2011; Dvorak et al, 2012; Carvalho et al, 2013; Carvalho et al, 2014; Santos-Alamillos et al, 2013; Garcia-Diez et al, 2012; Ji-Hang et al, 2014; Lundquist et al, 2014). The WRF model allows for accurate simulations of winds near the surface and at heights that are important for wind energy purposes. WRF's ability to downscale to resolutions of tens of meters allows the resolution of small-scale features, such as fronts, sea breezes, or winds influenced by orography, which are all important factors in describing the wind characteristics. WRF is thus an optimal tool to predict the distributions of the wind over a certain area, in this case Gujarat.

Downscaling allows a grid spacing of 1.1 km, finer than previous analyses. Likewise, increased temporal resolution with output every 10 minutes allows the calculation of highly resolved error metrics to validate our wind resource estimates. The results obtained in our study can therefore be used to help assess the accuracy of previous wind resource assessment studies for the area of Gujarat.

This report presents the results of the Gujarat wind resource assessment study. The WRF model, observations, and methods applied are described in Section 2. Results from a sensitivity study are presented in section 3. Section 4 covers wind resource maps based on yearly and monthly model simulations, a validation with observations, and a comparison with previous and other currently available resource assessments. Findings are summarized in section 5. The appendix provides additional graphs for the interested reader.

2 Data and Methods

WRF model simulations are validated with observations from five sites in Gujarat. This section describes the simulations, observations, the climate in Gujarat, and the validation process.

2.1 Mesoscale Model Simulations

The model simulations were carried out with the WRF model (Skamarock et al, 2008). WRF is a current-generation mesoscale numerical weather prediction system designed to serve both atmospheric research and operational forecasting needs (www.wrf-model.org). WRF features two dynamical cores, a data assimilation system, and a software architecture allowing for parallel computation and system extensibility. The model serves a wide range of meteorological applications across scales ranging from meters to thousands of kilometers. WRF is used operationally in the United States at the National Centers for Environmental Prediction (NCEP), the Air Force Weather Agency, and other centers. WRF is a community model that has been widely used for wind resource estimates as mentioned in the Introduction.

In WRF simulations the user has the choice of many different physical models that describe the interaction and processes between and in the land surface, the atmospheric boundary layer, and the middle and upper atmosphere. The physics options used for this study include the Lin et al. microphysics scheme, the Rapid Radiative Transfer Model for longwave radiation, the Dudhia scheme for shortwave radiation, the Eta similarity surface layer model, the Noah land surface model, the Mellor-Yamada-Janjic (MYJ) planetary boundary layer (PBL) scheme, the Yonsei University (YSU) PBL scheme, the quasi-normal scale elimination (QNSE) PBL scheme, and the Betts-Miller-Janjic cumulus parameterization. Land use categories come from the United States Geological Service (USGS).

Because modeling results are dependent on the inputs chosen by the user, a sensitivity analysis was carried out to yield the best model setup. That best model setup was then used to conduct the final one-year wind resource assessment. For the sensitivity analysis and the final simulations, atmospheric parameters were output every 10 min; except for one experiment in the sensitivity study, where it was every 1 min. That experiment served as a test for whether a higher temporal resolution would improve wind resource estimates. WRF output from every minute was then averaged to 10 minutes to see if that would yield more accurate wind estimates. The average was made from minute 6 to 14, thus centered around every 10 min to be comparable to the 10 min instantaneous output from the other experiments.

The WRF model is run at several different horizontal scales. These include a coarse outer domain, intermediate domains, and a finer-resolution inner domain. Feedback from the finer domains to the coarser domains was turned off for all simulations in order to study the effect of horizontal resolution in the two innermost domains. We used the nested setup to dynamically

downscale to 1.1 km in the finest domain (Figure 1). The grid spacings for each of the four domains are 33.3 km, 11.1 km, 3.3 km, and 1.1 km. In the finest domain, the number of grid points was 901 x 601. The 41 vertical levels for most sensitivity experiments and the year-long runs have their lowest model levels at 15 m, 47 m, 80 m, 112 m, 145 m, and 177 m above ground level (AGL). (Measurements of height are AGL unless otherwise noted.) The 69 vertical levels used for one experiment have their lowest model levels at 15, 36, 46, 57, 68, 78, 88, 99, 110, 120, 131, 141, 152, 162, 173, and 183 m.

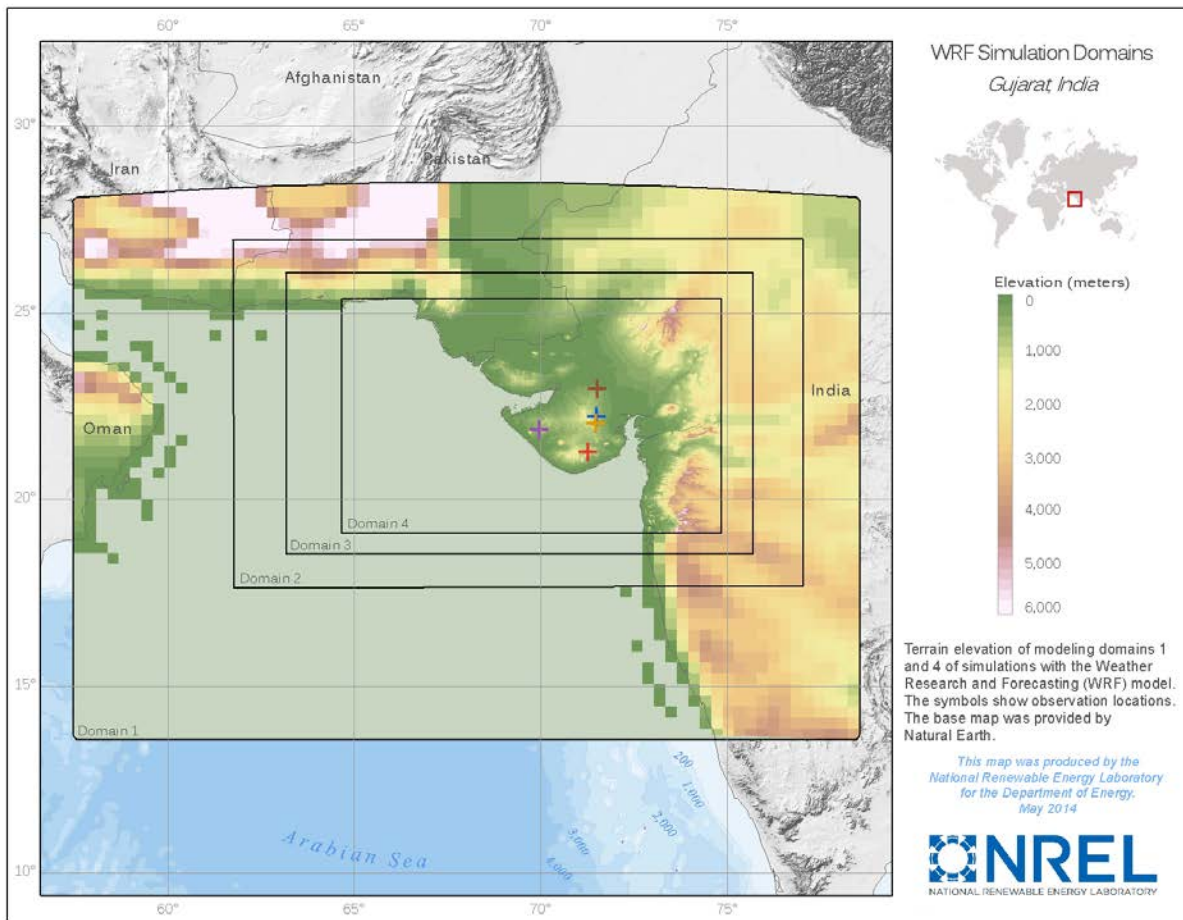


Figure 1. WRF simulation domains. Terrain elevation from domain 1 (33.3 km grid) is shown in domains 1–3, and from domain 4 (1.1 km grid) in domain 4. The crosses denote observation locations of the 5 measurement sites: purple - Balava, red - Jikiali, yellow - Virewa, blue - Sarva, brown - Jegawa.

The model was initialized at 00 UTC each day (which corresponds to 5:00 and 5:30 local time, depending on the location in India). The first 6 hours were regarded as model spin-up, so forecast hours 6–30 were used in the wind resource assessment and sensitivity studies. The model simulations are initialized and forced at the boundaries by 1/12 degree sea surface temperature (SST) fields and 1 degree U.S. NCEP Global Forecast System (GFS) analyses; one experiment was run with European Centre for Medium-Range Weather Forecasts (ECMWF) Re-Analysis (ERA-Interim) analyses at 0.7 degrees.

2.2 Observations

Observations at turbine hub heights are rarely made public. However, in Gujarat, data from five meteorological towers were available during 2011. The measured data were provided by the Centre for Wind Energy Technology (CWET). Model runs were validated with wind measurements from these towers, which were deployed across Gujarat (Figure 1 and Table 1). These towers measured wind speed and wind direction at 30 m and 50 m, and temperature at 10 m; the maximum and minimum values and standard deviation of these quantities were recorded as well. The latter were particularly useful in the quality control of the observations, which was carried out with the software Windographer (Windographer, 2014). We found through the quality control that the wind direction measurements of Sarva are dubious.

The observations were used for validation in both the six-week long sensitivity study and the one-year long wind resource assessment runs. The sensitivity analysis was carried out for three two-week periods in 2011, and the year-long simulations to estimate the wind resource assessment was run for the entire year 2011. The year 2011 was partly chosen because measurements from five towers were available to validate the wind resource modeled data.

Table 1: Observation Locations

Location	Latitude	Longitude
Balava	21.86906	69.96097
Sarva	22.22444	71.49161
Jegawa	22.95919	71.50833
Jikiali	21.27897	71.26333
Virewa	22.03747	71.46733

2.3 Climate in Gujarat

Knowledge about Gujarat's climate is important because the model validation should also look at how well the model captures climate characteristics. The Tropic of Cancer bisects Gujarat's northern border, leading to a tropical and subtropical steppe climate with occasional droughts and floods (National Disaster Management Authority of India, www.ndma.gov.in/en/gujarat-sdma-office). Cyclones occur occasionally along the coastline (Patel et al, 2011). Although most of Gujarat is flat, the northeast region of the state is covered by mountains and desert, with the highest elevation being 1,145 m.

While India has four seasons (winter, summer, monsoon, and post-monsoon), Gujarat has three primary seasons: winter, from November through March, summer from March through June, and the monsoon season from June (Pai et al, 2013) or sometimes May (Patel et al., 2011) through September. October is considered an intervening month. While the north region of Gujarat is arid and semi-arid, the southern region is humid. The seasonal cycle leads to strong winds from March through August and relatively weak winds from November through March. Because Gujarat has a long coast line, sea breezes also influence the wind characteristics in this region. The El Niño Southern Oscillation plays an important role in India. El Niño affects the monsoon. El Niño years are typically characterized by weak monsoons and droughts, whereas La Niña

typically leads to strong monsoons. According to the Indian Meteorological Institute, 2011 was characterized as a normal monsoon year in Gujarat—another reason this year was chosen for the assessment of the wind resource in addition to the availability of tower measurements at five sites across the state. 2011 was a moderate La Niña year for Gujarat, and the monsoon began on June 22 and concluded between September 23 and October 11, 2011.

2.4 Validation Methods

We validated the model simulations at five measurement stations across Gujarat. The validation includes visual and computational methods. Wind roses, frequency distributions, and time series of diurnal cycles and annual cycles provided a good visual aid in assessing model performance. Metrics used to validate the model were the root-mean-squared error (RMSE), bias, centered root-mean-squared error (CRMSE), the normalized RMSE to take the error dependency with wind speed into account (Drechsel et al, 2012), rank correlation, mean absolute error (MAE), wind distribution error (Windographer, 2014), and expected gigawatt-hours (GWh) per year (Table 2) with an example wind turbine with a 66-m rotor diameter. Observations were available only at 30 m and 50 m. Because current turbine heights are around 80 m and 100 m, metrics were computed at 80 m and 112 m. For 112 m the observations were extrapolated with the power law (Peterson and Hennessey, 1978) from 50 m to 112 m. For the long-term (one year) wind resource estimate, seasonal behavior (monsoon) and directional dependence were also analyzed.

The model output is 10-min instantaneous values, whereas the observations are 10-min averages. However, we do not expect the modeled variation of wind speed within 10 min to be significant enough to cause a major discrepancy to the observed average wind speeds. To minimize any potential concerns, the model was validated with hourly values as well. This also indicates whether the computational expense of having more frequent model output can be justified. Wind profiles were not evaluated because the maximum height of the measurements is only 50 m.

3 Sensitivity Study

The results of the WRF simulations are dependent on the inputs or the choices made by the user. Moreover, the more confidence there is in the configuration of the NWP model, the more valuable wind resource assessments are. Therefore, a sensitivity analysis was carried out to identify the best model setup. That best model setup was then used to conduct the final one-year wind resource assessment.

The main setup was motivated by a previous successful WRF modeling of wind resource estimates of the United States of America (Draxl et al, 2013). However, because the atmospheric peculiarities are different in Gujarat than in the United States, the WRF setup for the U.S.A. was taken only as a basis, and a sensitivity analysis was carried out.

Table 2: Error Metrics Used in the Analysis

Metric	Description
Root-mean-squared-error (RMSE)	$RMSE^2 = \frac{1}{N_p} \sum_{k=0}^{N_p} (F_k - O_k)^2 = CRMSE^2 + BIAS^2$; N_p is the number of available forecast (F) – observation (O) pairs. The $RMSE$ can be split into the systematic and random components ($BIAS$ and $CRMSE$) of the $RMSE$ (Taylor, 2001).
Bias (BIAS)	$BIAS = \bar{F} - \bar{O}$; \bar{F} and \bar{O} are the forecast and observation averages over N_p values. The bias is the systematic component of the error and describes the differences in the means of two time series.
Centered-root-mean-squared-error (CRMSE)	$CRMSE = \sqrt{\frac{1}{N_p} \sum_{k=0}^{N_p} [(F_k - \bar{F}) - (O_k - \bar{O})]^2}$; The CRMSE is the random component of the error, and describes the centered pattern of the error, the differences in wind speed variations around the mean.
Rank Correlation	The rank correlation reflects the strength of a monotone relationship between two variables.
Normalized RMSE	$RMSE/\bar{O}$; The RMSE is divided by the observation average over all the values.
Wind distribution error (WDE)	The WDE is a measure of how closely the distribution of wind speed of a set of predicted values matches the distribution of the observed values. $WDE = \sum_{k=0}^{Nf} \frac{(\hat{F}_i - F_i)^2}{F_i}$; Nf is the number of bins in the frequency distribution, F_i is the frequency of the i^{th} bin of the observed distribution, and \hat{F}_i is the frequency of the i^{th} bin of the predicted distribution (Windographer, 2014).

3.1 Model Setup

A sensitivity study was carried out to find the best model setup for the long-term high resolution model runs. For that purpose, WRF was run in hindcast mode for 2 weeks in each of the 3 seasons in Gujarat (i.e., 6 weeks), 1–15 Jan, 1–15 April, and 1–15 August. Eight different experiments were chosen to determine the best setup in terms of horizontal and vertical resolution, PBL scheme, temporal resolution, and boundary conditions. The different experiments are summarized in Table 3. The differences between the simulations of each experiment are listed in this table. All the simulations have the same first model level to exclude differences in output based on the lowest model level (Shin et al, 2012).

3.2 Results from Sensitivity Study and Implications

We evaluated the simulations at five measurement stations in Gujarat. The histograms for each of the five sites can be seen in Figure 2. In general, the tail of the model distributions shows higher values than observed, whereas in the center of the distribution, the modeled wind speeds are lower than observed. This results in a positive bias for all the stations and experiments. This behavior may be a result of the observed wind speeds being measured at 50 m, while the modeled data is for 80 m. WRF is also generally known to have a positive bias in wind speed at low levels, mainly because it underpredicts the frequency of light winds. It is also observed that the distribution from the simulations using the ECMWF ERA Interim data as boundary

conditions is very different and positively biased. The simulations using 69 vertical levels and the modeled wind speeds that were averaged to 10 min from 1 min model output show similar inaccuracies: distributions that are too wide and wind speeds that are too high. Using the wind distribution error, the simulations with experiment MYJ_41L perform best for 50-m wind speeds.

Comparing average diurnal cycles of wind speed and temperature (not shown), the experiments with 69 levels, ECMWF boundary conditions, and 1-min model output show the same behavior as described above, i.e., worse than the other experiments.

Wind roses for the observations show mainly three wind directions: southwest, northwest, and northeast (Figure 3 shows an example for Balava). The simulations with ECMWF boundary conditions miss the northwest component completely, while the runs using 1-min model output and 69 levels capture only the southwesterly component. All the other runs capture the wind direction signal satisfactorily.

Table 3. Experiments for Sensitivity Study

Experiment	Vertical Levels	Boundary Conditions	PBL Scheme	Output Frequency	Horizontal Grid Spacing
MYJ_41L	41	GFS	MYJ	10 min	1.1 km
MYJ_41L_ECMWF	41	ECMWF	MYJ	10 min	1.1 km
MYJ_41_1min	41	GFS	MYJ	1 min	1.1 km
QNSE_41L	41	GFS	QNSE	10 min	1.1 km
YSU_41L	41	GFS	YSU	10 min	1.1 km
MYJ_41L_3km	41	GFS	MYJ	10 min	3.3 km
MYJ_69L	69	GFS	MYJ	10 min	1.1 km

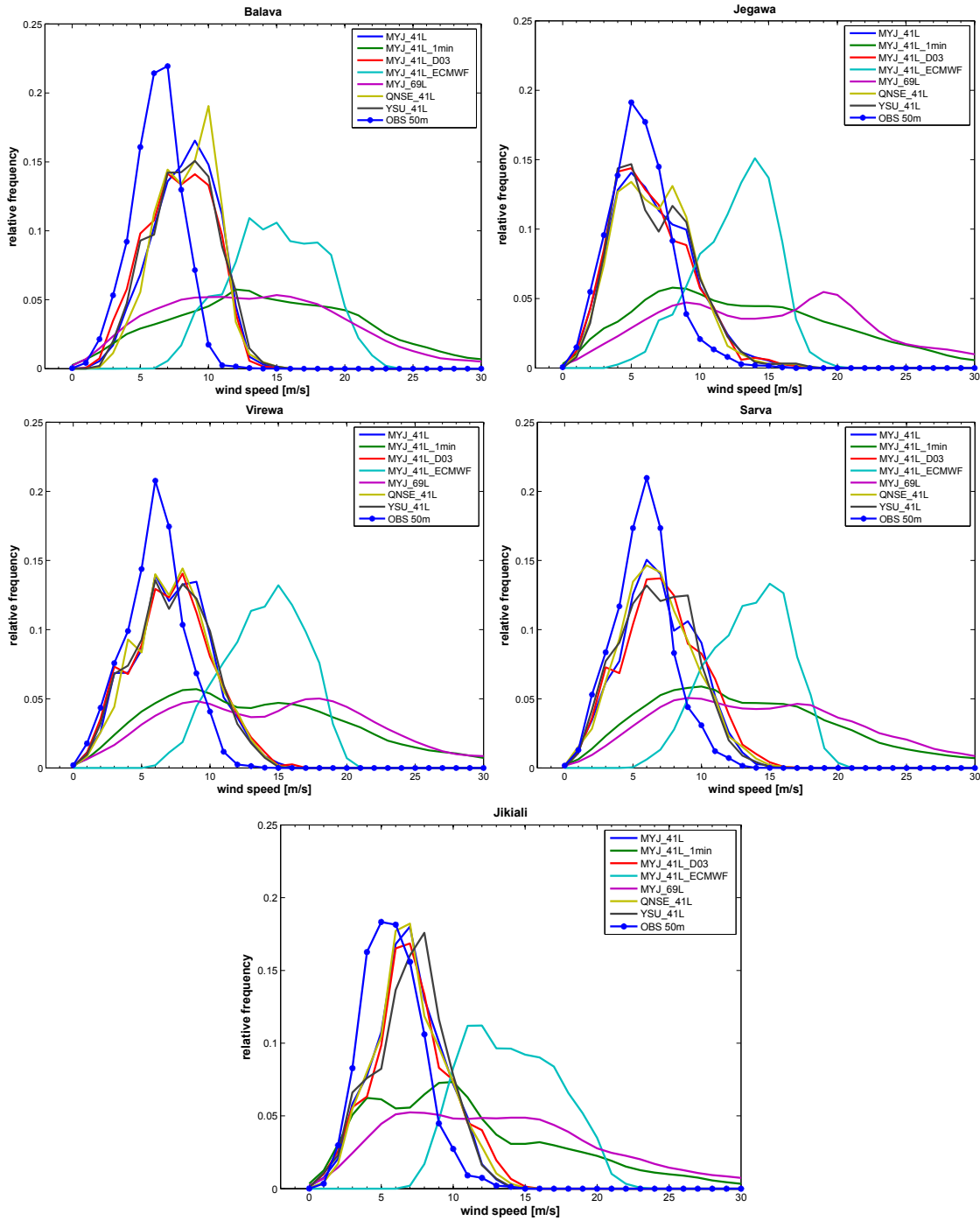


Figure 2: Histograms of wind speed for all the experiments and five locations, as indicated by the legend and title, respectively. Modeled wind speeds are at 80 m, observed at 50 m.

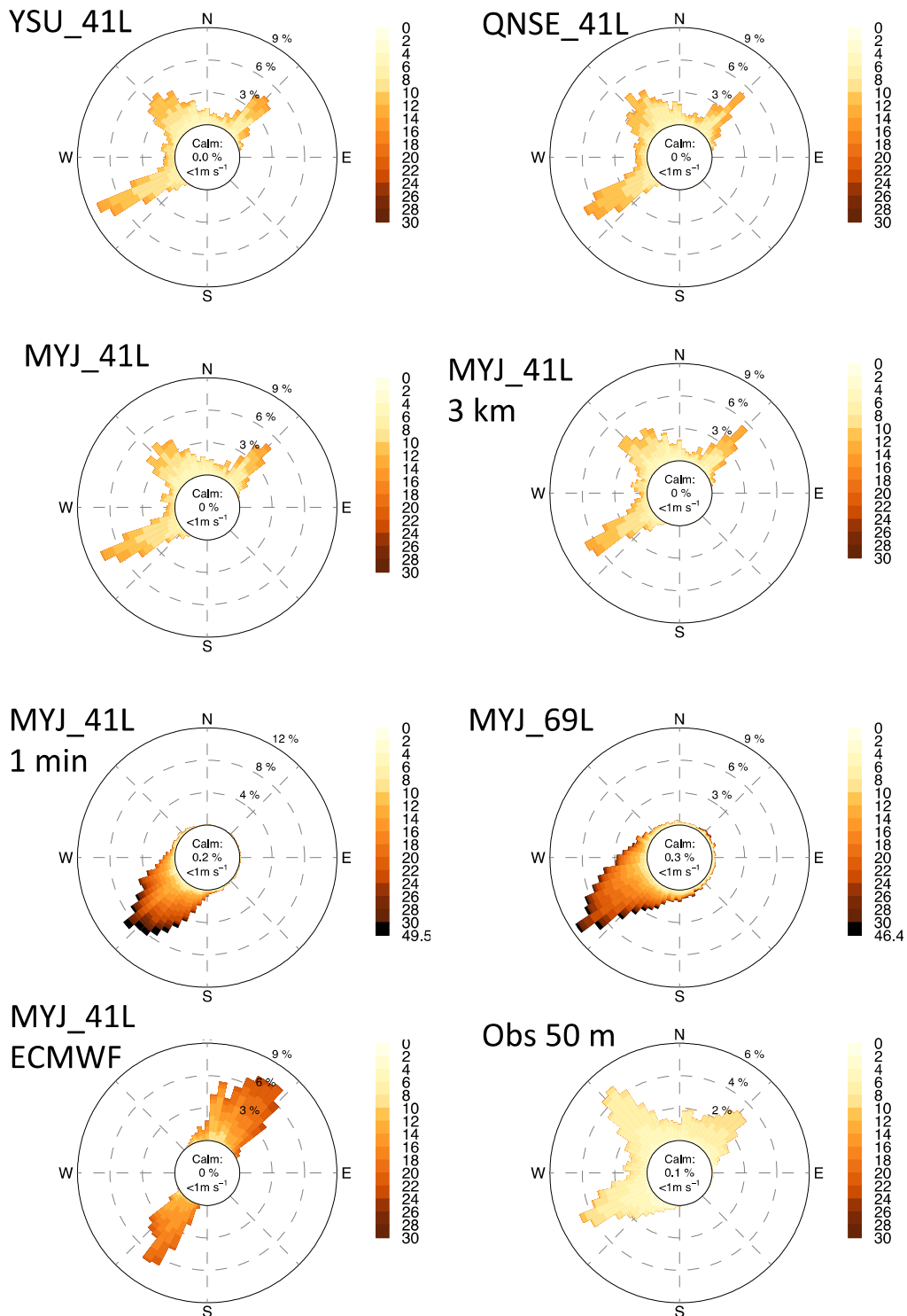


Figure 3: Wind roses for modeled wind speeds in meters per second at 112 m and observed at 50 m (bottom right) for Balava.

We further evaluated error metrics (RMSE, bias, CRMSE, rank correlation, and bias of potential GWh/year; bias is modeled minus observed wind speeds). The error metrics for experiments MYJ_69L, MYJ_41L_ECMWF, and MYJ_41L_1min are extremely bad as indicated by the histograms, with RMSE values on the order of 10 m/s. The experiments that performed the best are MYJ_41L, MYJ_41L_D03, and YSU_41L. A more detailed analysis was carried out among the three best performing experiments (Table 4 and Table 5).

Table 4. Error Metrics for the Sensitivity Study for 50 m Wind Speeds Averaged for All the Sites

Experiment	RMSE [m/s]	Bias [m/s]	CRMSE [m/s]	Correlation [-]	MAE [m/s]	Norm. RMSE [-]	WDE [-]	Bias [GWh/year]
MYJ_41L_D03	2.08	0.35	2.04	0.59	1.61	0.33	1403	0.53
MYJ_41L	2.04	0.37	1.96	0.58	1.60	0.32	1220	0.50
YSU_41L	2.03	0.42	1.95	0.59	1.58	0.32	1704	0.54

Table 5: Error Metrics for the Sensitivity Study for 112 m Wind Speeds Averaged for All the Sites.

Experiment	RMSE [m/s]	Bias [m/s]	CRMSE [m/s]	Correlation [-]	MAE [m/s]	Norm. RMSE [-]	WDE [-]
MYJ_41L_D03	2.68	1.20	2.38	0.63	2.11	0.39	7577
MYJ_41L	2.65	1.21	2.33	0.61	2.10	0.38	8233
YSU_41L	2.57	1.06	2.32	0.62	2.03	0.37	6663

The model runs using the MYJ PBL scheme and 41 vertical levels with a grid spacing of 3.3 km performed nearly as well as the runs using a grid spacing of 1.1 km. For the year-long runs we chose the 1.1-km grid spacing, because the error metrics were slightly better. For multi-year simulations or follow-up projects, a reassessment of additional value versus computational expense might be necessary for flat terrains like Gujarat. This finding is in line with current research, as model runs at a horizontal resolution of ~ 1 km do not necessarily produce more accurate results (as measured through point-wise metrics such as the ones we chose) than coarser resolution runs (Wyngaard, 2004). Research in this area should evaluate if ramping events or variability signals show differences, as mean error metrics tend to be favored by coarser grid spacing. The WRF setup was motivated by wind resource studies in the United States and optimized for 41 levels. We suggest that increasing the number of levels to 69 might have altered the background static stability, which resulted in poorly performing simulations.

The simulations using the YSU boundary layer scheme performed slightly better during low winds (0–3 m/s) using the RMSE, bias, MAE, and rank correlation. Taking the wind speeds into account that are most important for wind energy (i.e., 3.5–25 m/s), the wind distribution error, and the potential GWh/year using the whole wind speed range, the MYJ PBL scheme outperformed all the other schemes. Because the differences in error metrics between the YSU and MYJ PBL scheme are very small (tenths of meters per second), and the MYJ PBL scheme has an option for turbulence kinetic energy output that might be relevant for future studies, we

used the MYJ boundary layer scheme to model the wind resource for one year. These simulations have a horizontal grid spacing of 1.1 km, 41 vertical levels, and use GFS boundary conditions.

4 Gujarat's Wind Resource

Based on the validation results from the sensitivity study, the WRF was run for the year 2011 with 41 vertical levels and the MYJ PBL scheme. GFS data and sea surface temperatures were used as boundary conditions (experiment MYJ_41L in Table 3). The model output from domain 4 with a 1.1-km grid spacing serves as the basis for the wind resource estimate for Gujarat. Data were converted into monthly and annual average wind speeds for each point on the grid, as required.

4.1 Results

A hub height of greater than 80 m would most likely be better for energy production given the obstructions and thick ground cover in Gujarat. However, the deployment of turbines with a hub height closer to 80 m will be likely in the near term due to the current high costs of turbines with taller hub heights and any regulations that may limit the height of turbines. This report presents the annual averages of wind speed at both 80 m and 112 m and the monthly averages at 80 m only.

Figure 4 to Figure 6 show maps of average horizontal wind speed for the State of Gujarat, including the area 20 miles off the coast that might initially be explored for offshore wind energy. Several aspects influence the wind distribution in a region, such as topography, land cover, distribution of land and sea, and atmospheric pressure gradients. Therefore there may be local variations that are not captured in these maps. In general, offshore wind speeds are higher than those on land, which is similar to conditions in Europe and the United States.

Considering the usual seasonal cycle that can be expected in India (section 2.3) and the validation results at the five measurement sites (section 4.2), the wind speed is highest in the summer from May to August, with maximum average wind speeds exceeding 10 m/s, especially along the coasts. The wind speed is lowest in October and November with average wind speeds not exceeding 7 m/s at coastal sites.

Annual average wind speeds at 112 m above the surface are higher than at 80 m (Figure 4 and Figure 5). Average annual wind speeds at 80 m reach 8 m/s around the coast. The majority of the Gulf of Khambhat experiences annual averages of 6-7 m/s. At specific sites on the mainland, especially in northwest Gujarat and north of the north coast of the Gulf of Kutch, wind resources are abundant.

Depending on the turbine type, wind resources are usually viable for wind energy applications at annual average wind speeds greater than approximately 6 m/s. For wind turbines with larger rotors, lower wind speeds become viable. That lower limit for wind resource assessment may change with future advances in wind turbine technology.

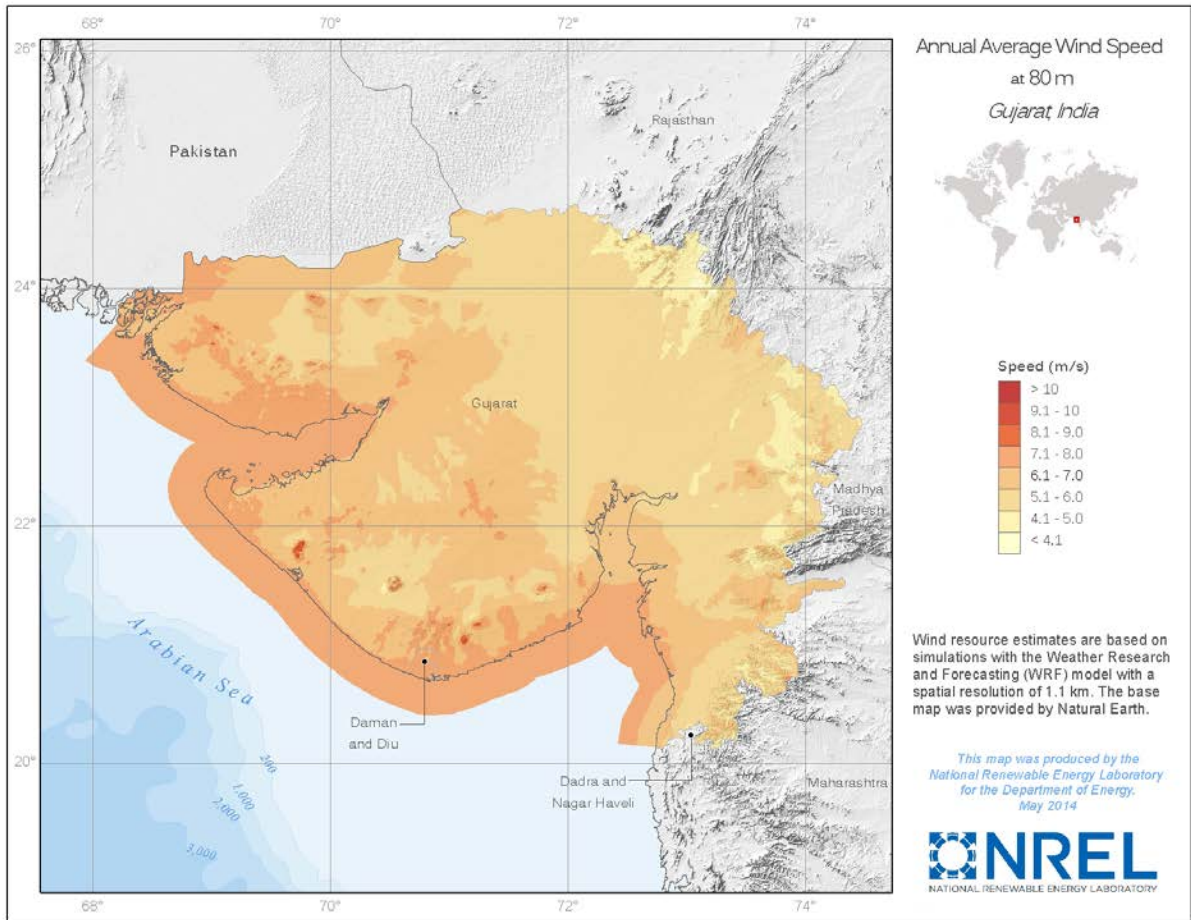


Figure 4: Annual average wind speeds at 80 m.

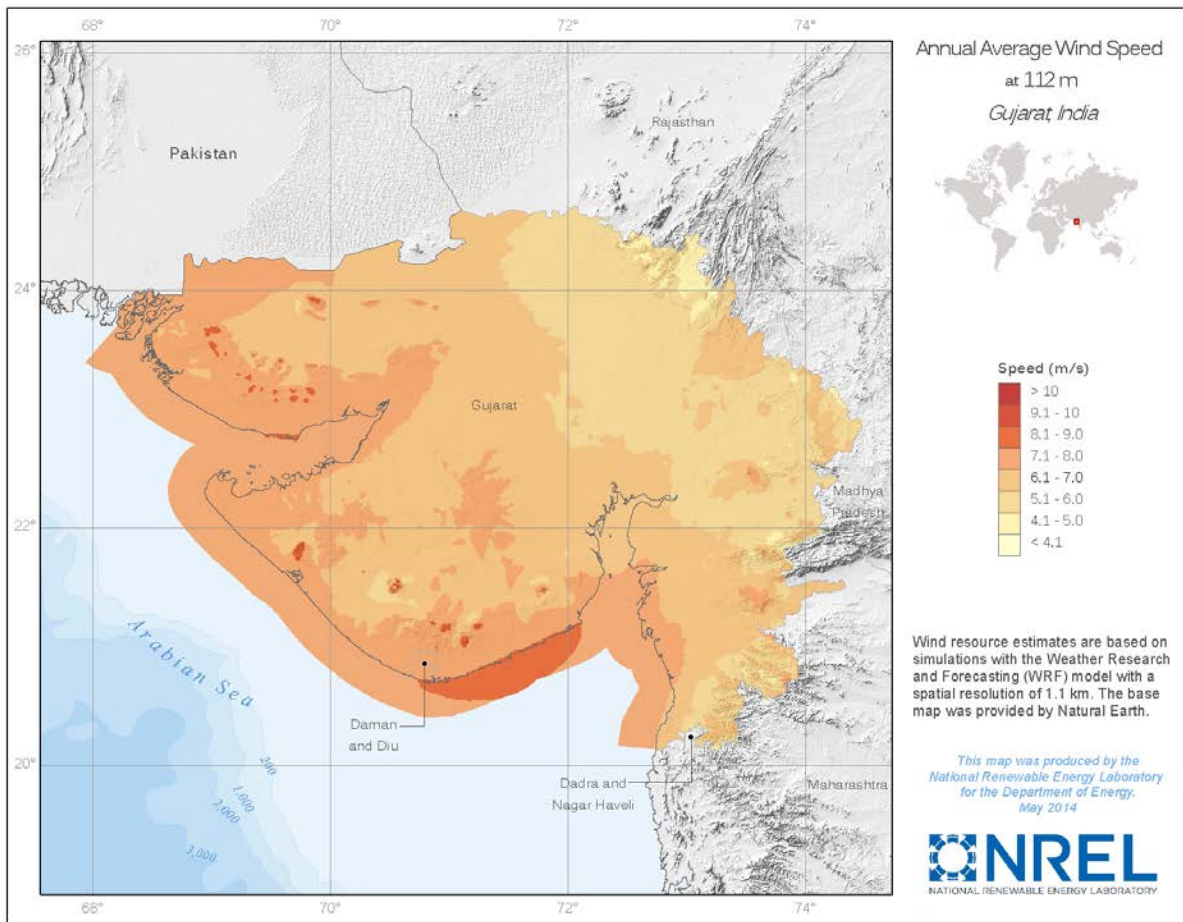


Figure 5: Annual average wind speeds at 112 m.

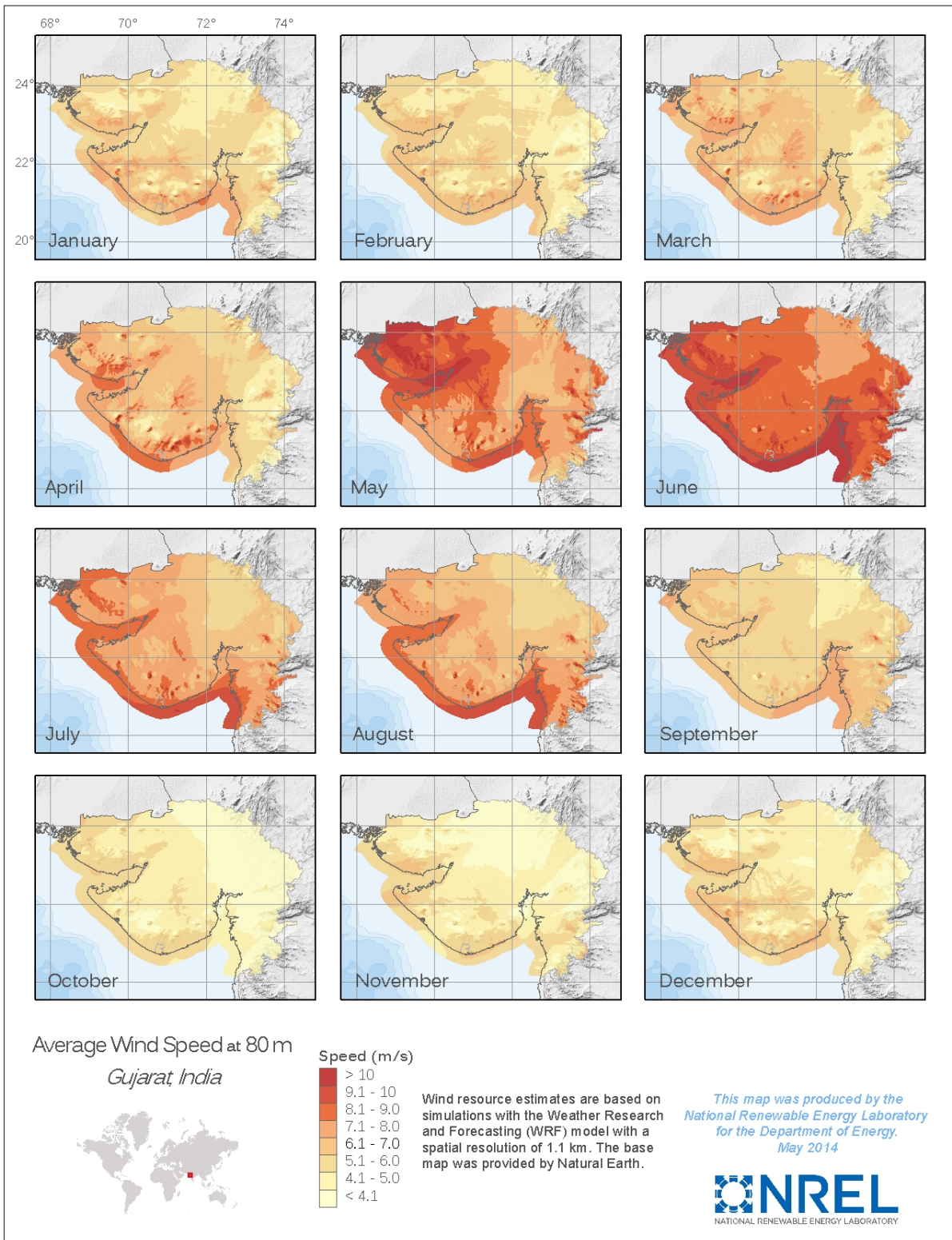


Figure 6: Average wind speeds for every month during 2011.

4.2 Wind Resource Validation

The one-year-long model simulations were compared to measurement data from five measurement sites throughout Gujarat. This enabled an estimate of the model performance and validation of the wind resource estimate. This validation gives a good indication of whether our wind maps can be trusted. Because the measurements were only available at 10 m and 50 m, we validated the model with the 50-m measurements.

The validation includes various aspects:

- a) Temporal resolution: Usually, NWP models used for wind resource assessment produce output every hour at the most. We ran our NWP model producing 10-min output to determine if a higher temporal resolution would lead to more accurate results.
- b) Diurnal cycles: In addition to yearly bias and RMSE, we were interested in whether or not the model was able to capture a diurnal cycle in wind speed, which is associated with the transitions from a stable PBL at night to a convective PBL during the day.
- c) Seasonal and annual cycles: Because India's seasons are greatly influenced by the monsoon, we wanted to see if the model reproduces seasonal signals in the data. This was checked using with wind roses and annual cycles.

These aspects are discussed in detail in the following sections.

4.2.1 Histograms

In general, the frequency distributions of the simulated wind speeds at 50 m correspond well with those observed at all the five sites (Figure 7). WRF tends to exhibit lower frequencies in the peak region between 4 and 8 m/s and to overestimate wind speeds at the right tail of the distribution.

4.2.2 Error Metrics

For the 10-min instantaneous modeled and 10-min sustained observed wind speeds, the RMSE is approximately 2 m/s at all the sites. The normalized RMSE is around 0.4. According to our experience, this is a reasonable result for NWP modeling. This RMSE can be decomposed in the CRMSE and the bias. The bias is mostly positive for all the sites except for Jikiali, where it is very slightly negative. Balava has the highest bias (0.73 m/s), followed by Virewa with a bias of 0.52 m/s. The other sites have biases lower than 0.1 m/s. The biggest part of the RMSE constitutes the CRMSE, which describes the random component of the error and the intrinsic skill of the model. CRMSE ranges are between 1.83 and 2 m/s. The rank correlation shows reasonable values for all the sites, and the MAE reaches values between 1.5 and 1.6 m/s. The lowest wind distribution error is at Jegawa, the highest at Balava. Figure 7 confirms these results.

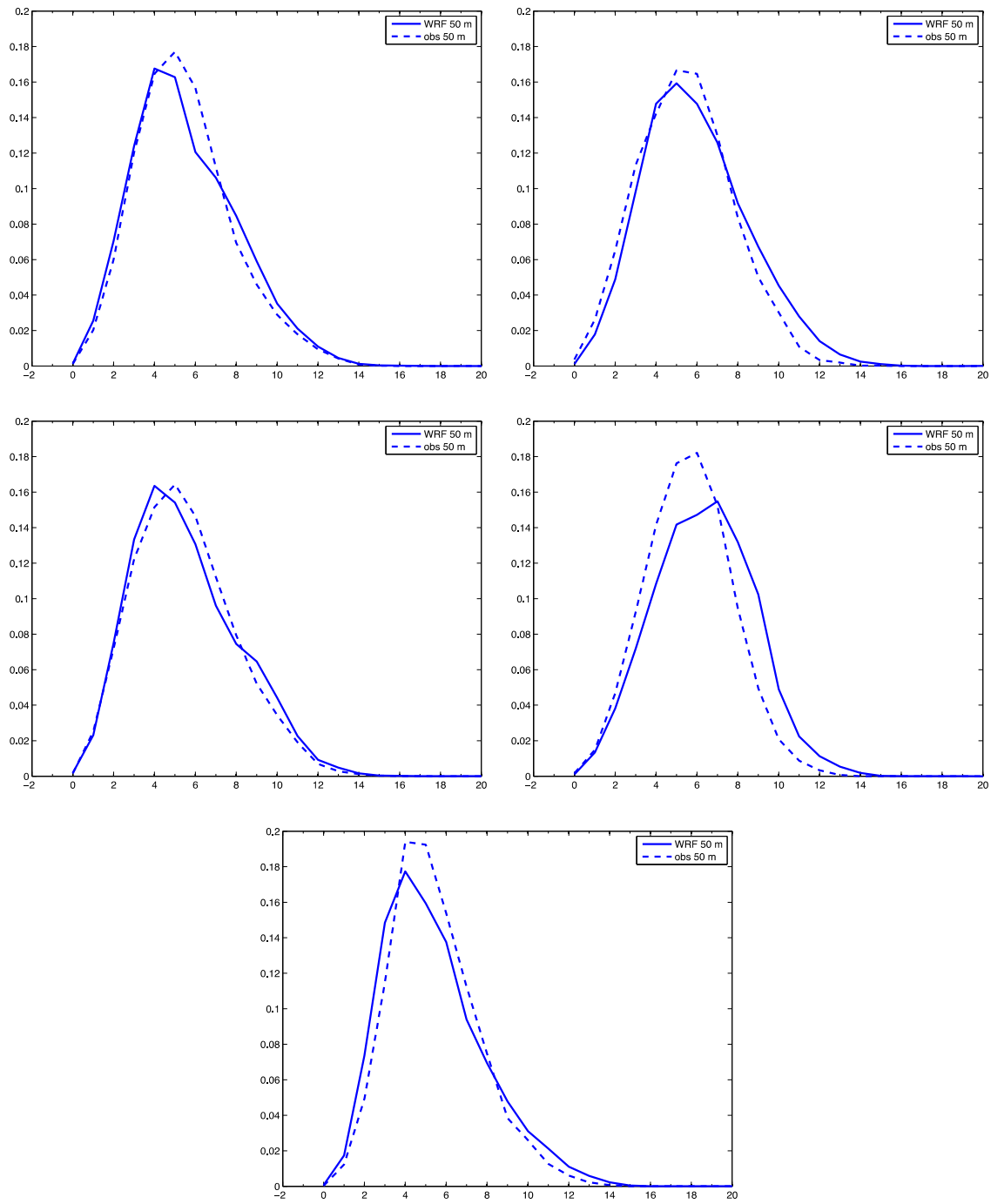


Figure 7: Histograms of observed (dashed lines) and simulated (solid lines) wind speed at 50 m at the five measurement sites as indicated in the title of each panel.

Table 6. Error Metrics for 2011 for 10-min Model Output for 50 m in meters per second

Site	RMSE [m/s]	Bias [m/s]	CRMSE [m/s]	Correlation [-]	MAE [m/s]	Norm. RMSE [-]	WDE [m/s]
Balava	1.98	0.73	1.83	0.67	1.55	0.35	13,510
Jikiali	1.93	-0.03	1.93	0.58	1.57	0.36	3,806
Sarva	2.01	0.09	2.00	0.63	1.51	0.37	1,199
Virewa	1.98	0.52	1.91	0.62	1.56	0.36	6,727
Jegawa	1.97	0.08	1.97	0.67	1.47	0.36	898

4.2.3 Impact of Temporal Resolution

Because NWP models used for wind resource assessment usually produce hourly outputs, we examined whether high temporal resolution data, i.e., outputs every 10 min, would lead to more accurate results. As expected, using hourly values gives lower but similar error metrics (Table 7). For hourly model output the CRMSE was slightly reduced. This leads to a lower RMSE as well. The rank correlation values were degraded for hourly output, but the MAE decreased. The normalized RMSE is about the same. The WDE decreased considerably. This degradation might be due to the fact that instantaneous hourly model output is not representative of intra-hourly wind variations that would be captured with 10-min model output. This is a very positive aspect of using high temporal resolution data. The overall wind resource estimate was not altered significantly by using 10-min instead of hourly data. For future projects, using hourly data for wind resource estimates might suffice for sites with a climate similar to that of Gujarat.

Table 7. Error Metrics for 2011 for Hourly Model Output for 50 m in Meters per Second. (A more detailed breakdown of RMSE and bias into diurnal cycles per month for all the 5 stations is in the appendix, Figure 28 through Figure 37).

Site	RMSE [m/s]	Bias [m/s]	CRMSE [m/s]	Correlation [-]	MAE [m/s]	Norm. RMSE [-]	WDE [m/s]
Balava	1.81	0.77	1.64	0.68	1.45	0.34	783
Jikiali	1.85	-0.67	1.72	0.44	1.56	0.35	924
Sarva	1.77	0.11	1.76	0.57	1.28	0.33	252
Virewa	1.91	0.34	1.88	0.60	1.55	0.32	253
Jegawa	1.86	0.02	1.86	0.51	1.39	0.34	118

4.2.4 Diurnal Cycles

Diurnal cycles of simulated wind speed at 10 m, 50 m, 80 m, and 112 m and for observed wind speeds at 10 m and 50 m are shown in Figure 8 for Jegawa. Diurnal cycles for the other locations are shown in the appendix. The data were averaged for every hour. Plots of diurnal cycles allow for a more detailed analysis of how well the model captures transitions from stable to convective boundary layers and diurnal variations throughout the day. The diurnal cycles are very well captured at most sites at 50 m.

Diurnal cycles of modeled temperature, atmospheric stability, and boundary layer height, and of observed temperature were qualitatively examined (not shown). Results appeared reasonable.

As expected, wind speeds are lower during a convective boundary layer during the day than at night, when low-level jets might increase wind speeds above 50 m. On the contrary, wind speeds near the surface at 10 m are lower during the night. Observed winds at 10 m are mostly overpredicted throughout the day, which might also be due to measurement errors or sensors being installed in non-representative locations. Diurnal cycles of wind speeds at 50 m correspond very well to those observed, except for Jikiali and Balava. These two locations are closest to the ocean and might be influenced by land-sea breezes.

4.2.5 Wind Roses

Because the simulated wind direction at 50 m does not differ considerably from that at 80 m, wind roses with observed directions at 50 m are compared to those simulated for a potential hub height of 80 m in Figure 9.

The wind roses capture the wind directions very well. The simulated wind direction signal show a stronger southwest signal than observed for all stations but Sarva. These wind roses are the combined wind signals for 2011. A breakdown per month for all the locations shows a strong monthly signal of usually one dominant wind direction (see data for Balava in Figure 22 and Figure 23 in the appendix). The strong southwest summer monsoon and weaker northeast winter monsoon can be seen clearly. The modeled wind directions correspond very well to the observed ones, which can be seen as an indication that the model captures seasonal signals. The slight overprediction of modeled wind speeds is seen through the darker colors in the modeled wind roses.

4.2.6 Annual Cycle

Figure 10 shows annual cycles of simulated wind speed at Sarva at 50 m, 80 m, and 112 m, and observed wind speeds at 50 m in the first panel; wind speed bias for winds at 50 m (simulated minus observed) in the second panel; and normalized RMSE of wind speeds at 50 m in the third panel. Annual cycles for all the other stations can be found in the appendix (Figures 24–27).

At all locations, the modeled wind speed increases with height, and WRF tends to underpredict wind speeds in the winter and overpredict them in the summer. For Balava, WRF overpredicts in all the months except October and November. This overprediction in the summer is also reflected in the bias, which is highest in the summer and lower in the winter at all the sites. It is therefore mostly negative during winter months and positive during summer months. That cycle is also visible for Balava, although the bias is only negative during October and November. At Virewa, November, December, and April are the only months with a slightly negative bias, and similar to other locations, the bias is highest in a summer month. Biases are mostly below 1 m/s, except for Virewa in June and July and Balava from May until August.

The RMSE values are similar at all locations, and like the bias, the annual cycle of RMSE exhibits lower values during the winter (not shown). Because wind speeds are higher during the summer and high RMSE values during high winds might be an artifact, we show the normalized RMSE (by observed wind speed) in each plot. The normalized RMSE is highest during October and November for all locations (except Balava) and lowest in early summer.

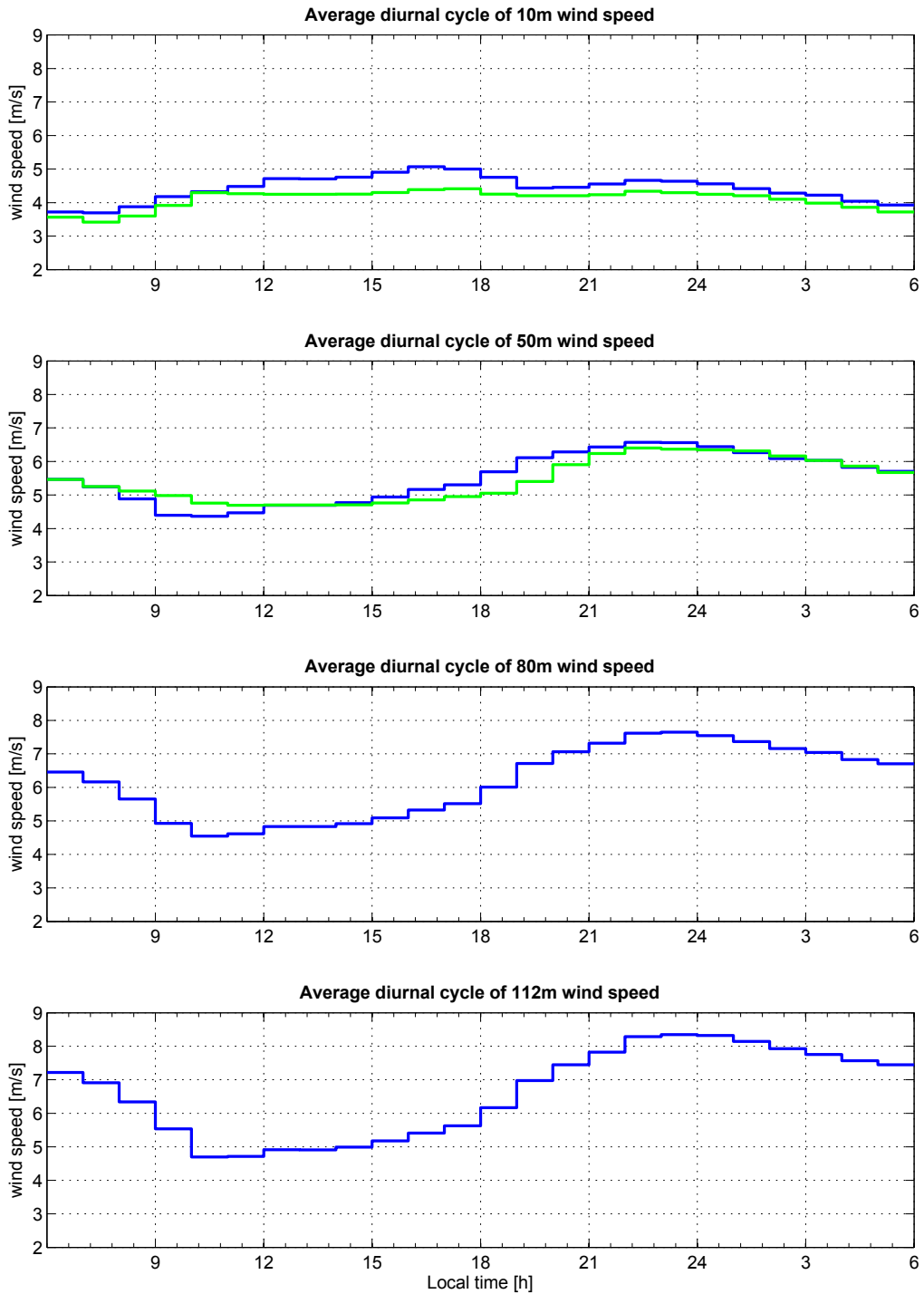


Figure 8: Average diurnal cycle of wind speeds at different heights for Jegawa as indicated in the panel titles. Simulated wind speeds are in blue, observed in green.

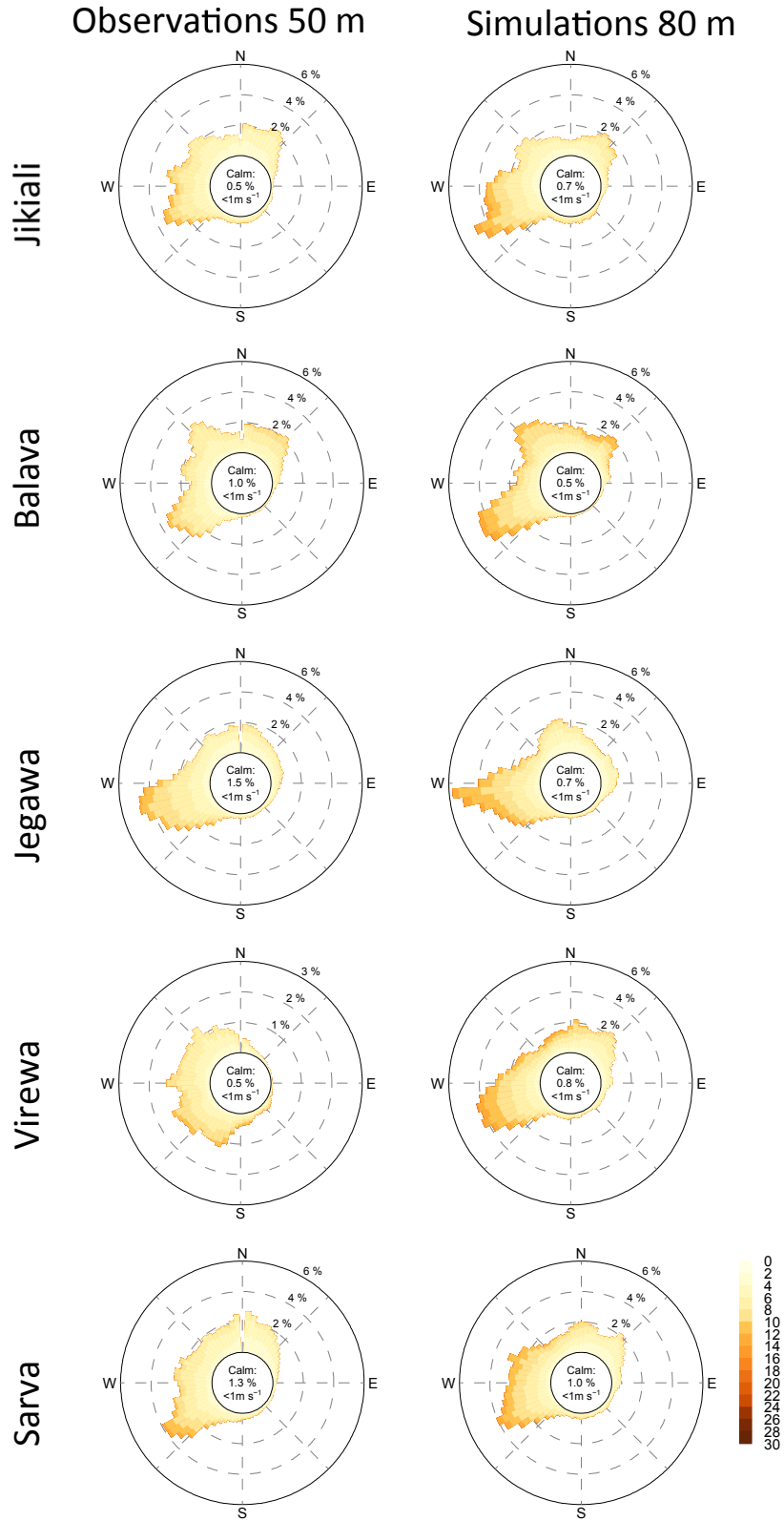


Figure 9: Wind roses for observed wind speeds in meters per second at 50 m (left column) and simulated wind speeds at 80 m (right column) for the five measurement sites.

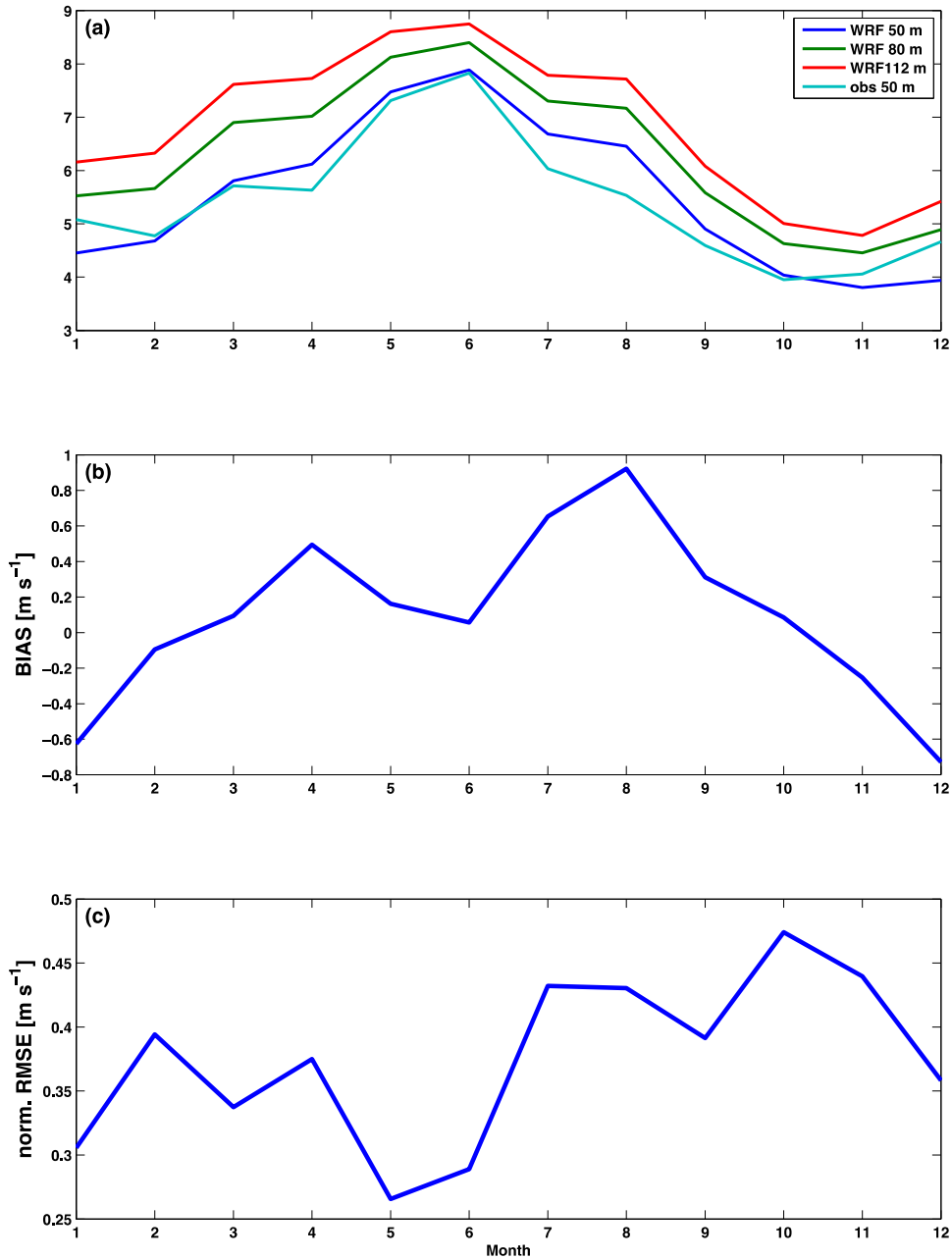


Figure 10: Sarva's annual cycle of simulated wind speed at 50 m, 80 m, and 112 m, and observed wind speeds at 50 m (panel a), wind speed bias for winds at 50 m (simulated minus observed; panel b), and normalized RMSE of wind speeds at 50 m (panel c).

Apart from a monthly/seasonal signal in wind direction (see section above), we show histograms and wind speed time series per month in the Appendix to estimate wind resources in different months and to evaluate the model's capability of capturing annual cycles. Figure 13 to Figure 17 (in the appendix) show that the modeled wind speed frequency in each month is generally similar to the observed wind speed frequency. However, during some months the observed distributions do not follow the modeled ones.

4.3 Comparisons of Simulations with Existing Wind Resource Estimates for Gujarat

This analysis adds to the existing literature by using the WRF model to estimate wind resource in Gujarat at 80 m and 112 m. The WRF model has been used in previous estimates as well, but with a lower temporal and horizontal resolution. While previous publications show the wind power density over the whole country, this report presents maps indicating wind speed, which in turn can be transformed to wind power densities using various methods.

Phadke et al. (2011) found that Gujarat is one of the states with the highest wind energy potential, most of which is concentrated in the northwestern part of the state north of the Gulf of Kutch. In our analysis, the yearly average for 2011 shows the highest potential at the same location but also shows a similarly high potential along the south coast of the peninsula (offshore and on the coast between Sarakhadi Gam and Gadhula).

The following maps are available from CWET (Gomathinayam and Boopathi, 2014). Qualitatively, the areas of highest wind resource in Gujarat agree with our findings (Figure 11).

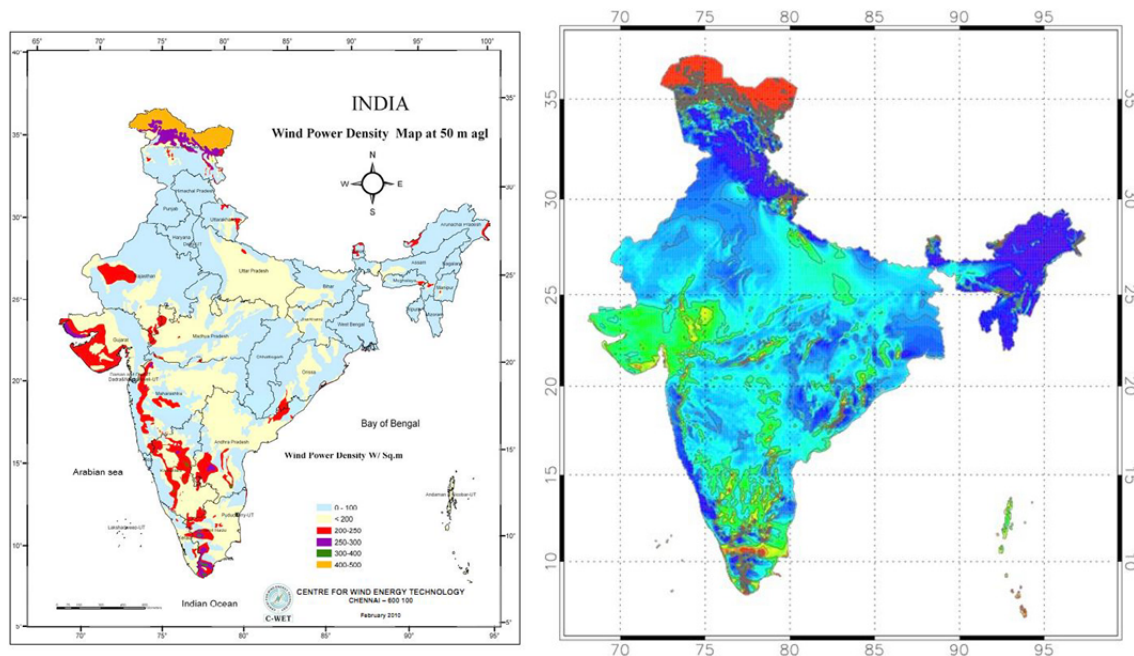


Figure 11: Wind power density at 50 m (left) and 80 m (right). From CWET (CWET 2014).

The International Renewable Energy Agency (IRENA, 2014) publishes worldwide wind maps. A 5-km gridded onshore wind speed estimate is available for Gujarat at 80 m above ground. According to IRENA, these data were provided by 3TIER. A screenshot of the IRENA estimate is shown in Figure 12.

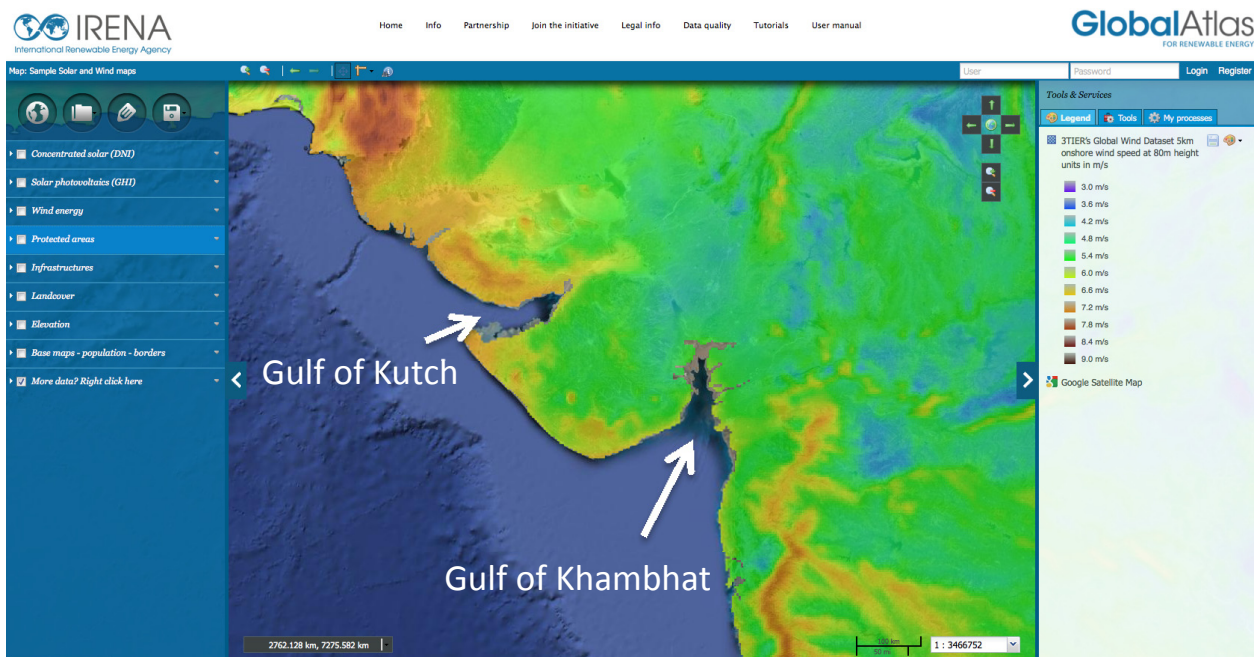


Figure 12: Screenshot of wind speed estimates from Irena (<http://irena.masdar.ac.ae/?map=178>, accessed May 2014).

According to the IRENA map, the highest wind resource is again in the Gulf of Kutch, but also in the Gulf of Khambhat, followed by the northwest of Gujarat and the southern tip of the peninsula. This corresponds to findings presented here of wind speeds between 6 and 7 m/s near the coasts, and maximum average winds of 9 m/s. We did not identify the Gulf of Khambhat as having the high wind potential indicated by IRENA.

Recent ground measurements performed by CWET indicate that the wind speed north of the Gulf of Kutch may be higher than the wind speeds modeled in our study (K. Boopathi, CWET, personal communication, June 2014). However, these ground measured data were not available for comparison in this analysis.

5 Summary and Conclusion

A wind resource assessment for the Indian state of Gujarat has been carried out. This resource assessment was made using the WRF model and validated against data from five sites across Gujarat. WRF was chosen because of its applicability to a wide range of atmospheric conditions, and successful use for resource estimates in other locations. Furthermore, we wanted to make the results reproducible by using a model with open access. The model setup was chosen based on previous modeling experiences and the domain setup was constrained by computational limits.

Prior to the year-long simulations, we carried out a sensitivity study using two weeks each in January, April, and August 2011. This sensitivity study therefore covers the main seasons, and serves to find the optimal boundary conditions, grid spacings, and physics settings in the model that give the most accurate results for Gujarat. The sensitivity study showed that finer horizontal resolution results in better resource estimates, but that the increase in accuracy between a grid spacing of 1.1 km and 3.3 km is minor, and therefore might not be worth the additional

computational expense. Error metrics between these two grid spacings were similar. We further investigated whether a temporal resolution of 1 min, 10 min, or 1 hour would yield best results for wind energy estimates. We found that averaging 1-min WRF model output to 10 min resulted in worse and inaccurate wind speeds. Hourly model output resulted in slightly better error metrics. Again, the higher computational expense to create higher temporal resolution model output is not worth the effort. We therefore used 10-min model output for the year-long simulations. We further found that the ERA Interim boundary conditions yield very poor wind speed estimates. This is surprising in that the ERA Interim is known to produce more accurate results in Europe (Carvalho et al, 2013). For the Indian subcontinent however, we recommend using GFS boundary conditions.

We compared our simulations to measurements at five locations throughout Gujarat. We validated the simulations against observations using traditional error metrics such as RMSE, MAE, and bias; we also used rank correlation, CRMSE, normalized RMSE, and the wind distribution error. Annual and diurnal cycles of wind speed, wind roses, and histograms of wind speed shed further light onto the behavior of the WRF model. Although highly relevant in wind energy, we refrained from analyzing wind profiles, because observations were only available at 10 m and 50 m. Instead, we offer wind maps at 80 m and 112 m. Sudden changes in wind speed (ramp events) and variability are important for grid integration purposes, but were not taken into account either, as grid integration topics are beyond the scope of this study.¹

Validation results showed a very good agreement between modeled and observed winds. A small positive bias was found, leading to an estimated overprediction of less than 0.8 m/s for the annual average. These and the other results presented in this report are very encouraging and give us confidence in an accurate wind resource assessment.

For the future, error estimates would add high value to wind resource maps. Those can be done without access to additional observations. Methods to estimate the uncertainty of the wind resource include ensembles, using data assimilation techniques and/or adjoints. Statistical methods that relate the one-year runs to long-term estimates such as the Analog Ensemble method (Delle Monache, 2013) or the Bias Correction Spatial Disaggregation method (Wood et al. 2004) could be employed to yield a long-term resource characterization of approximately 20 years.

Previous analyses of the wind resource in India, and specifically near Gujarat, indicated a wide range of estimates. This report aims at providing a further estimate to reduce the ambiguity of past estimates. While previous resource assessments presented wind power density, our report focuses on average wind speeds, which can be converted to wind power densities by the user with methods of their choice.

Our wind resource estimate corresponds to existing estimates and shows regions with average annual wind speeds of more than 8 m/s. These areas are concentrated in the Gulf of Kutch and on the south coast of the peninsula. Consistent with the usual seasonal cycle in India and with the

¹ NREL is currently conducting a wind grid integration analysis for Gujarat. The report is scheduled to be published in fall 2014.

validation results at five measurement sites, the wind speed is highest in the summer from May to August with maximum average wind speeds of higher than 10 m/s, especially along the coast lines. The wind speed is lowest in October and November with average wind speeds not exceeding 7 m/s at coastal sites. The topography, land cover, and distribution of land and sea result in varied winds in Gujarat. In general, offshore wind resources are higher than those on land, as expected. Annual average wind speeds are higher at 112 m than at 80 m.

References

- Amin, A. L. (1999). Liberalization of the Indian power industry: Wind power in Gujarat. *Renewable Energy*, 16(1-4), 977-980. doi:10.1016/S0960-1481(98)00345-0.
- Bakshi, R. (2002). Wind energy in India. *IEEE Power Engineering Review*, 22(9), 16–18. doi:10.1109/MPER.2002.1029967.
- Carvalho, D.; Rocha, A.; Gómez-Gesteira, M.; Silva Santos, C. (2014). WRF wind simulation and wind energy production estimates forced by different reanalyses: Comparison with observed data for Portugal. *Applied Energy*, 01/2014, 117, 116–126.
- Carvalho, D.; Rocha, A.; Silva Santos, C.; Pereira, R. (2013). Wind resource modelling in complex terrain using different mesoscale–microscale coupling techniques. *Applied Energy*, 2013, vol. 108, issue C, pages 493–504.
- Dvorak, M.J.; Corcoran, B. A.; Hoeve, J.E.T.; McIntyre, N.G.; Jacobson, M.Z. (2012). US East Coast offshore wind energy resources and their relationship to peak-time electricity demand. *Wind Energy*, 16, 977–997. doi: 10.1002/we.1524.
- Centre for Wind Energy Technology, last accessed May 2014:
http://www.cwet.tn.nic.in/html/information_isw.html, last accessed May 2014.
- Centre for Wind Energy Technology (2010). Indian Wind Energy Atlas.
http://www.cwet.tn.nic.in/docu/Indian_wind_atlas_brochure.pdf, last accessed May 2014.
- Delle Monache, L.; Eckel, T.; Rife, D.; Nagarajan, B. (2013). Probabilistic weather prediction with an analog ensemble. *Monthly Weather Review*, 141, 3498–3516.
- Draxl, C.; Hodge, B.M.; Orwig, K.; Jones, W.; Searight, K.; Getman, D.; Harrold, S.; McCaa, J.; Cline, J.; Clark, C. (2013). *Advancements in Wind Integration Study Data Modeling: The Wind Integration National Dataset (WIND) Toolkit*. National Renewable Energy Laboratory, Golden, CO. USA. NREL/CP-5D00-60269.
- Draxl, C.; Hahmann, A.N.; Peña, A.; Giebel, G. (2012). Evaluating winds and vertical wind shear from Weather Research and Forecasting model forecasts using seven planetary boundary layer schemes. *Wind Energy*. doi: 10.1002/we.1555.
- Drechsel, S.; Mayr, G.J.; Messner, J.W.; Stauffer, R. (2012). Wind speeds at heights crucial for wind energy: measurements and verification of forecasts. *J. Appl. Meteor. Climatol.*, 51, 1602–1617. doi: <http://dx.doi.org/10.1175/JAMC-D-11-0247.1>.
- Garcia-Diez, M.; Fernandez, J.; Fita, L.; Menendez, M.; Mendez, F.J.; Gutierrez, J.M. (2012). Using WRF to generate high resolution offshore wind climatologies. *8^o Congreso Internacional AEC*, Salamanca, Spain, Sep. 2012. Proceedings.

Gomathinayagam, S., Boopathi, K. India's National Initiatives and Experiences related to wind resource assessment. Power Point presentation available from:
<http://www.google.com/url?sa=t&rct=j&q=&esrc=s&source=web&cd=1&ved=0CCgQFjAA&url=http%3A%2F%2Fwww.irena.org%2Fmenu%2F.%255CDocumentDownloads%255Cevents%255C DelhiEvent%255C1.4%2520CWET%2520wind%2520mapping.pdf&ei=aUhyU5XIENKhyAS0i4DwDA&usg=AFQjCNF7fudzbbzI-9meulJyyZNCxtTOwQ&bvm=bv.66699033,d.aWw>.
Last accessed May 2014.

International Renewable Energy Agency (IRENA):
http://www.irena.org/DocumentDownloads/Publications/GWEC_India.pdf, last accessed May 2014

Jagadeesh, A. (1987). Integration of wind farms into the public power system in India. *Adv in Windfarming, Proc of the Int Conf and Exhib on Windfarms, October 13, 1987 - October 16, 1987*, 27(1-3), 433–438.

Jagadeesh, A. (1985). Economic feasibility of power generation with windmills in India – a case study. *European Wind Energy Conference 1984: Proceedings of an International Conference, EWEC '84*, 708–713.

Jaswal, A.K.; Koppar, A.L. (2013). Climatology and trends in near-surface wind speed over India during 1961–2008. *Mausam*, 64(3), 417–436.

LI Ji-Hang; GUO Zhen-Hai; WANG Hui-Jun (2014). Analysis of wind power assessment based on the WRF model. *Atmospheric and Oceanic Science Letters*, 7(2): 126–131.

Lundquist et al (2014). Estimating the wind resource in Uttarakhand: comparison of dynamic downscaling with Doppler lidar wind measurements. NREL Technical report NREL/TP-5000-61103.

National Disaster Management Authority of India, (2014) <http://www.ndma.gov.in/en/gujarat-sdma-office>, last accessed May 2014.

Mani, A.; Mooley, D.A. (1986). Wind Energy Data for India, Allied Publishers Private Limited, 545 pp.

Mooley, D.A. (1983). Wind characteristics and wind power potential of the Indian summer monsoon. *Mausam*, 34(1), 9–26.

Patel, H. N.; Porey, P. D.; Manekar, V. L. (2011). Proposed offshore wind farm planning at Kalpasar project, Gujarat, (India) Asia. *2nd Annual Conference on Electrical and Control Engineering, ICECE 2011, September 16, 2011 - September 18, 2011* (pp. 5385–5388). IEEE Computer Society. doi:10.1109/ICECENG.2011.6058152.

Phadke, A.; Bhavirkar, R.; Khangura, J. (2011). *Reassessing Wind Potential Estimates for India: Economic and Policy Implications*, September 2011. Report LBNL-5077E.

- Peterson, E. W.; Hennessey, J. P. (1978): On the Use of Power Laws for Estimates of Wind Power Potential. *J. Appl. Meteor.*, **17**, 390–394. doi: [http://dx.doi.org/10.1175/1520-0450\(1978\)017<0390:OTUOPL>2.0.CO;2](http://dx.doi.org/10.1175/1520-0450(1978)017<0390:OTUOPL>2.0.CO;2)
- Rao, K.S. (1986). Renewable Energy in India. *Electricity Conservation Quarterly*, **6**(3),7–8.
- Santos-Alamillos, F. J.; Pozo-Vázquez, D.; Ruiz-Arias, J. A.; Lara-Fanego, V.; Tovar-Pescador, J. (2013). Analysis of WRF model wind estimate sensitivity to physics parameterization choice and terrain representation in Andalusia (Southern Spain). *J. Appl. Meteor. Climatol.*, **52**, 1592–1609. doi: <http://dx.doi.org/10.1175/JAMC-D-12-0204.1>.
- Shin, H. H.; Hong, S; Dudhia, J. (2012). Impacts of the lowest model level height on the performance of planetary boundary layer parameterizations. *Mon. Wea. Rev.*, **140**, 664–682. doi: <http://dx.doi.org/10.1175/MWR-D-11-00027.1>.
- Skamarock, W.C.; Klemp, J.B.; Dudhia, J.; Gill, D.O.; Barker, D.M.; Duda, M.G.; Huang, X.Y.; Wang, W.; Powers, J.G. (2008). *A description of the Advanced Research WRF Version 3*. NCAR Tech Notes-475+STR. Boulder, CO: National Center for Atmospheric Research.
- Storm, B.; Basu, S. (2010). The WRF Model forecast-derived low-level wind shear climatology over the United States Great Plains. *Energies*, **3**, 258–276. doi:10.3390/en3020258.
- Taylor, K. E. (2001). Summarizing multiple aspects of model performance in a single diagram. *J. Geophys. Res.*, **106**, 7183–7192. doi:10.1029/2000JD900719.
- Tyagi, A. and Pai, D.S. et al (2012). Monsoon 2012 – A report. Technical report Synoptic Meteorology No.1/2012. Government of India – India Meteorological Department.
- Windographer, <http://www.windographer.com>, last accessed May 2014.
- Wood, A.; Maurer, E.P.; Kumar, A.; Lettenmaier, D.P. (2002). Long range experimental hydrologic forecasting for the eastern United States. *Journal of Geophysical Research*, **107** (D20): 4429. doi:10.1029/2001JD000659, 2002.
- Wyngaard, J.C. (2004). Toward numerical modeling in the “Terra Incognita.” *J. Atmos. Sci.*, **61**, 1816–1826. doi: [http://dx.doi.org/10.1175/1520-0469\(2004\)061<1816:TNMITT>2.0.CO;2](http://dx.doi.org/10.1175/1520-0469(2004)061<1816:TNMITT>2.0.CO;2).

Appendix

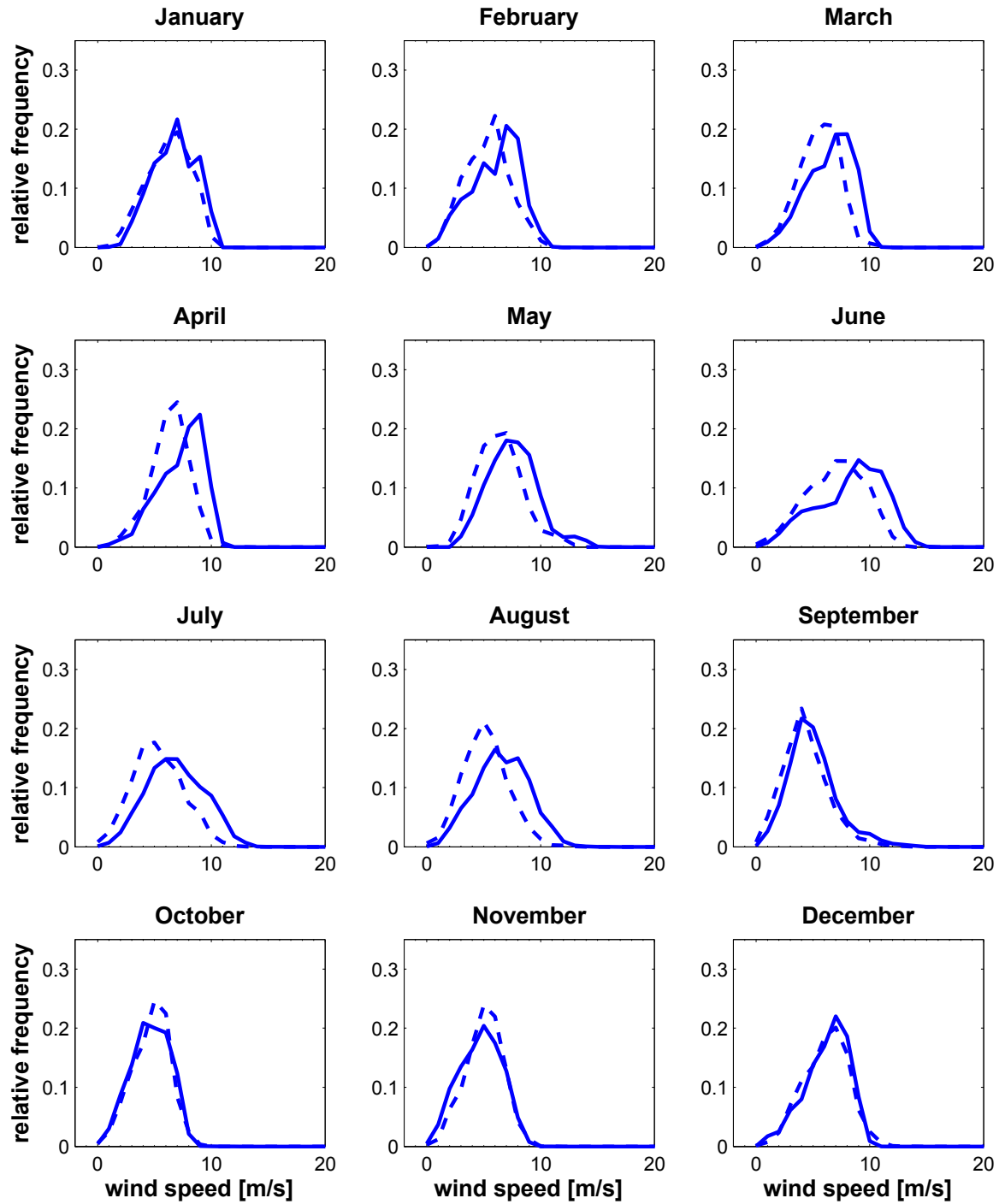


Figure 13: Histograms for each month in 2011 of 50 m observed (dashed lines) and simulated (solid lines) wind speeds for Balava

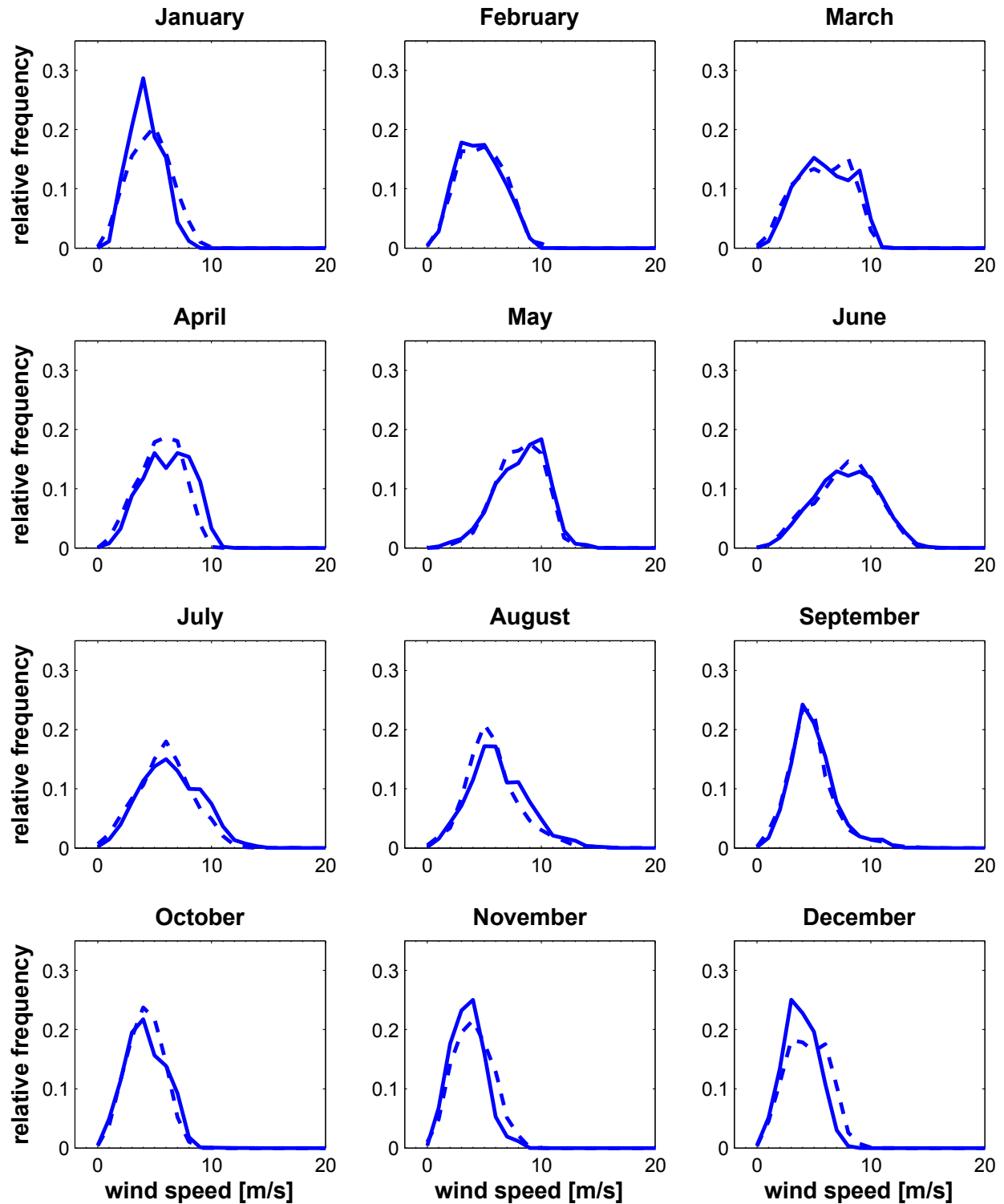


Figure 14: Histograms for each month in 2011 of 50 m observed (dashed lines) and simulated (solid lines) wind speeds for Jegawa.

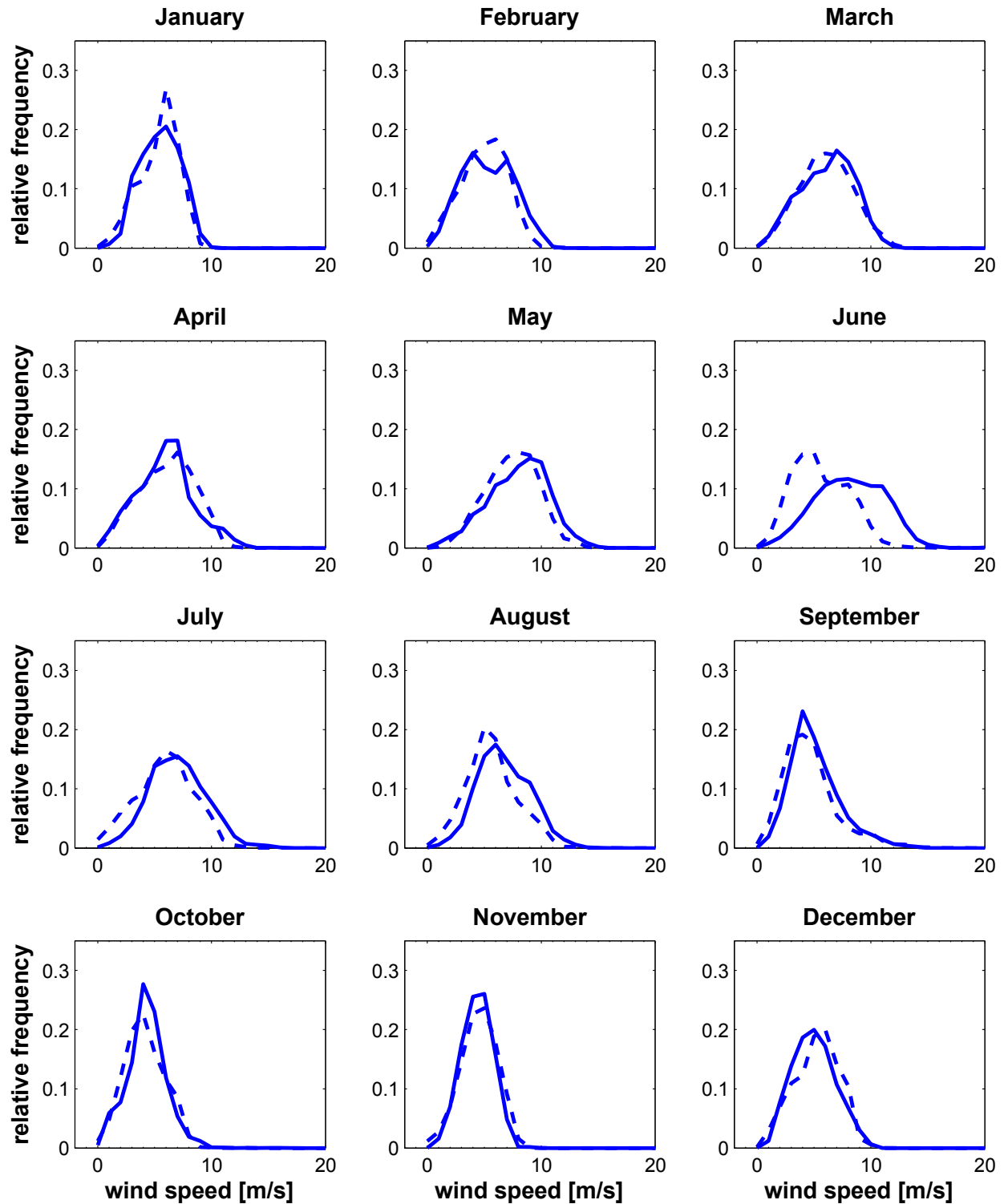


Figure 15: Histograms for each month in 2011 of 50 m observed (dashed lines) and simulated (solid lines) wind speeds for Virewa.

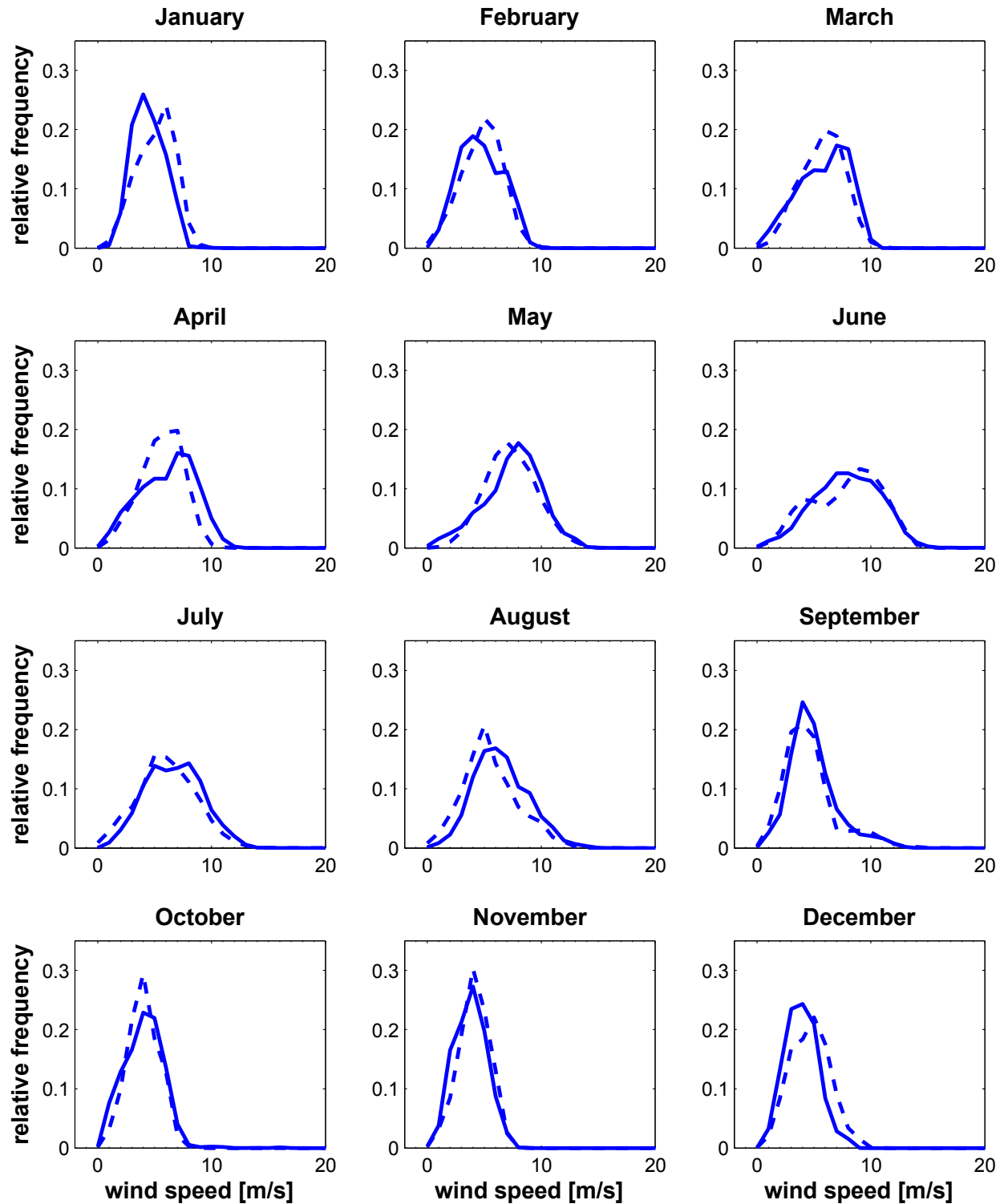


Figure 16: Histograms for each month in 2011 of 50 m observed (dashed lines) and simulated (solid lines) wind speeds for Sarva.

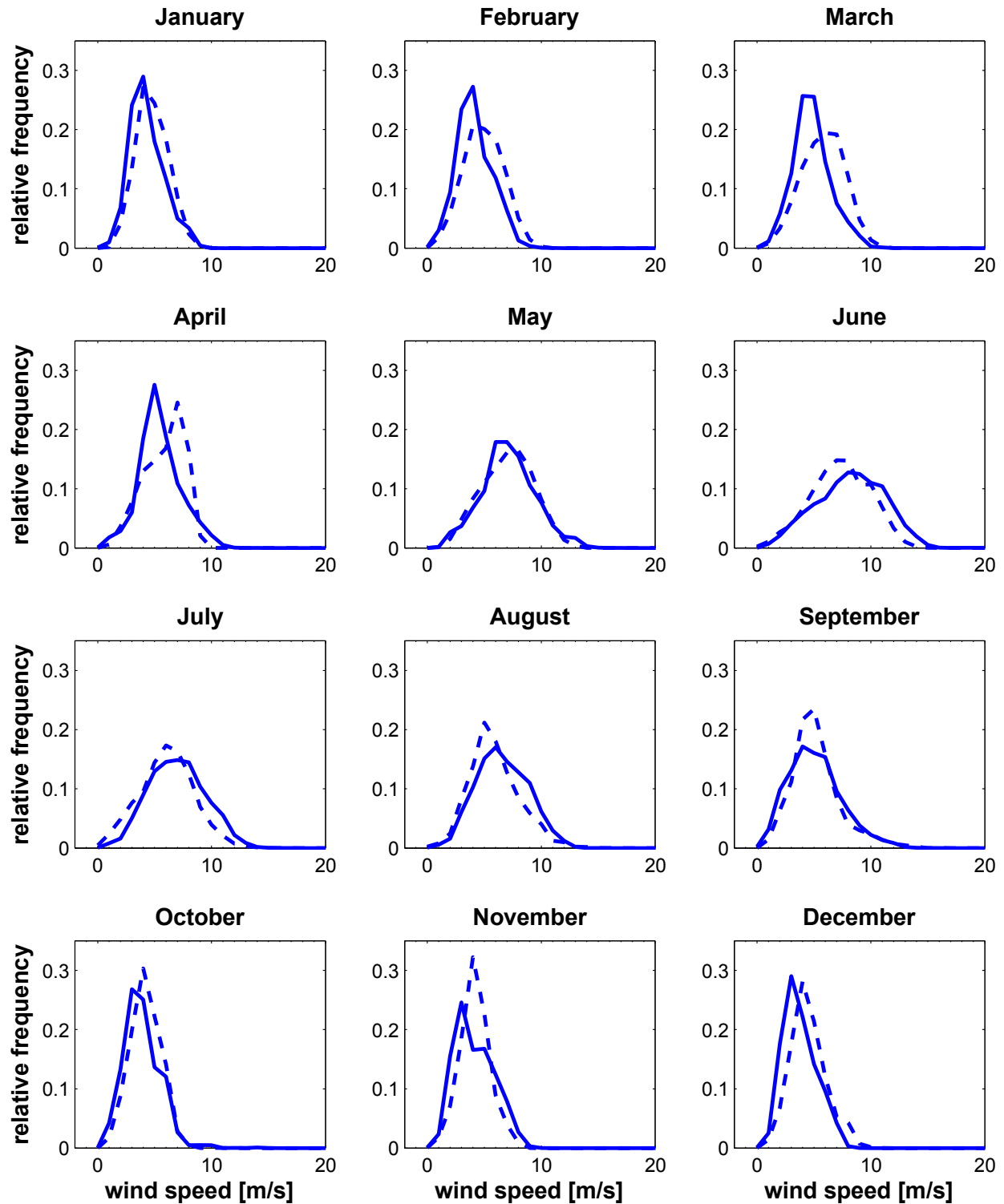


Figure 17: Histograms for each month in 2011 of 50 m observed (dashed lines) and simulated (solid lines) wind speeds for Jikiali.

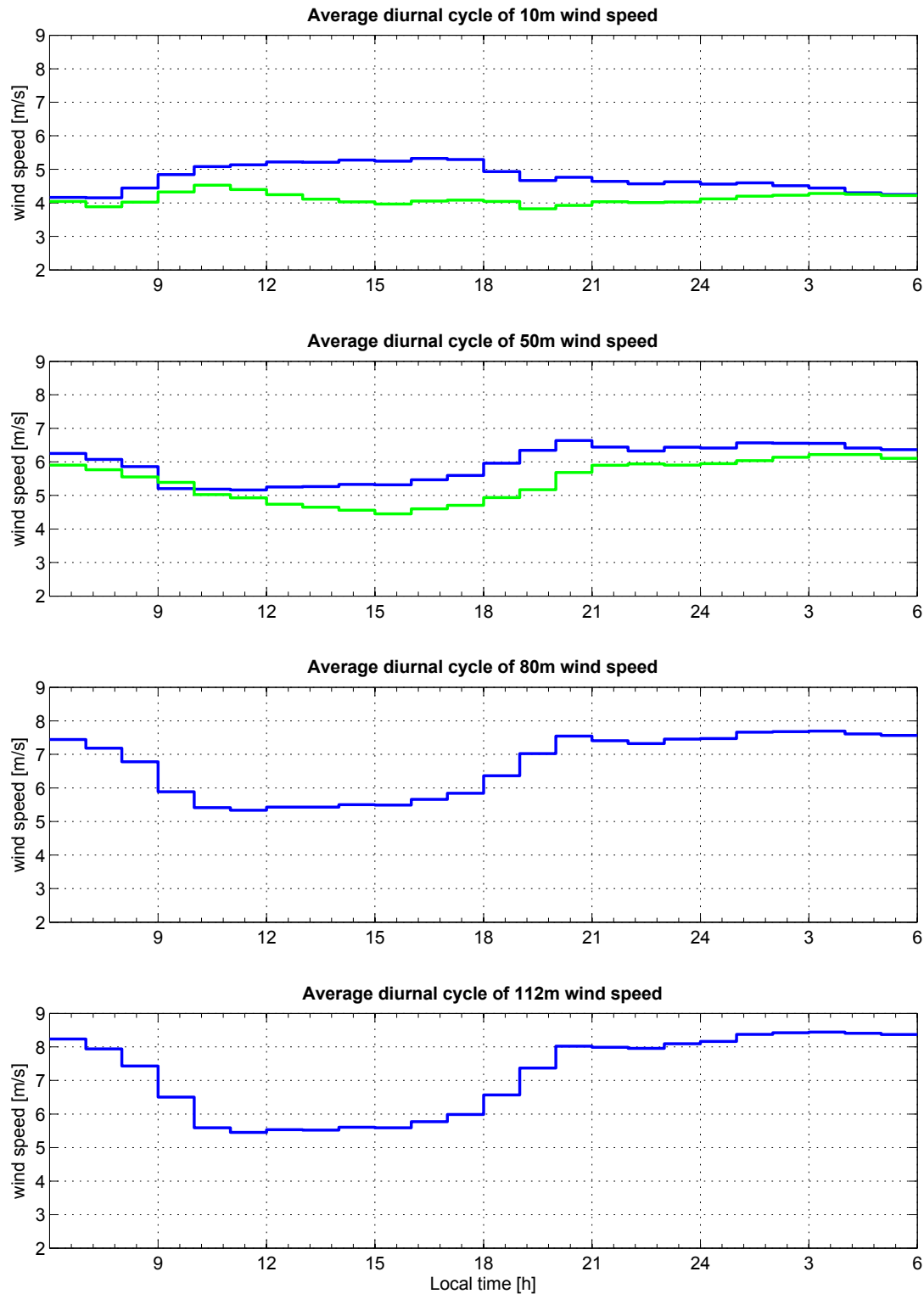


Figure 18: Average diurnal cycle of wind speeds at different heights as indicated in the panel titles for Virewa. Simulated wind speeds are in blue, observed in green.

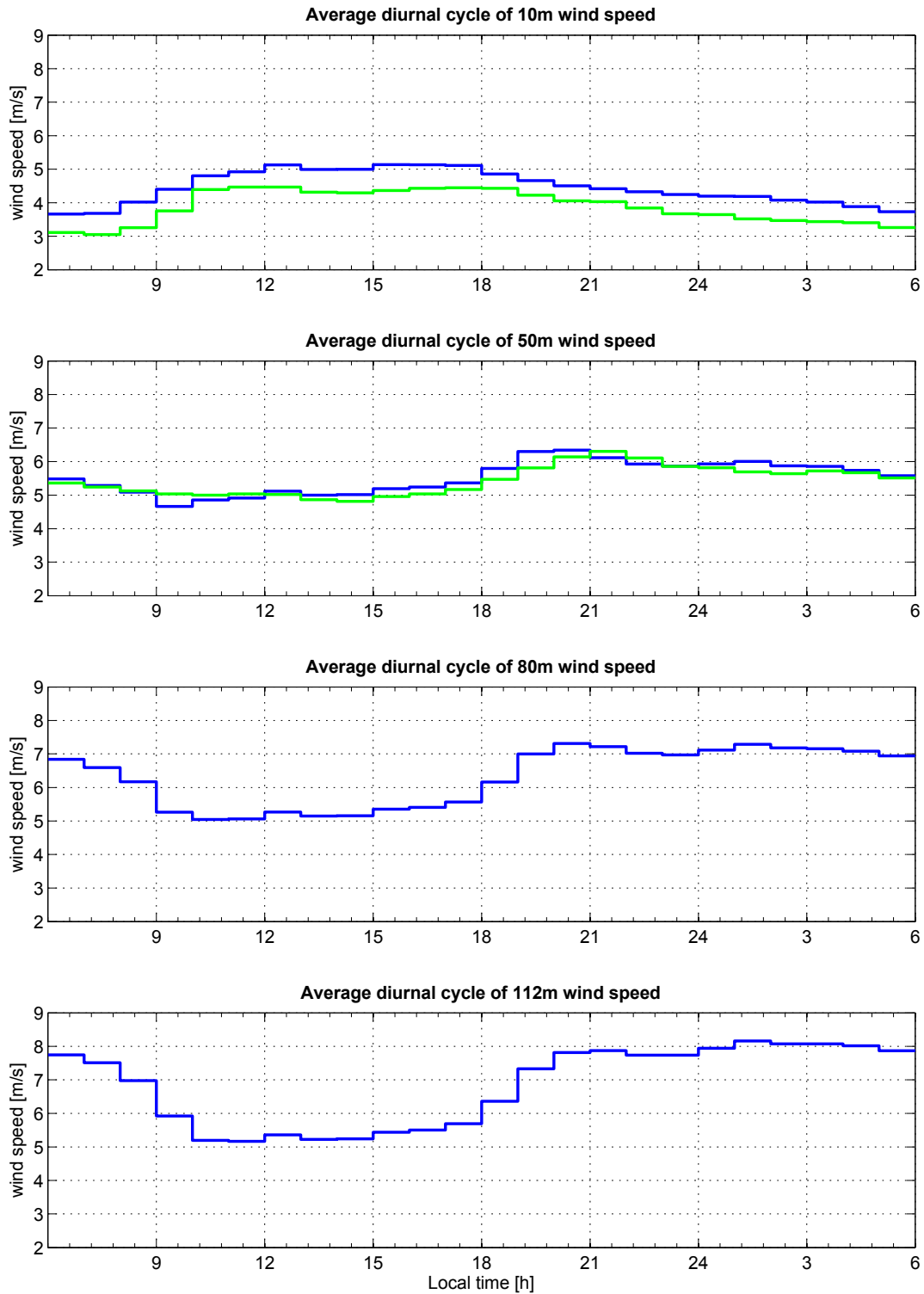


Figure 19: Average diurnal cycle of wind speeds at different heights as indicated in the panel titles for Sarva. Simulated wind speeds are in blue, observed in green.

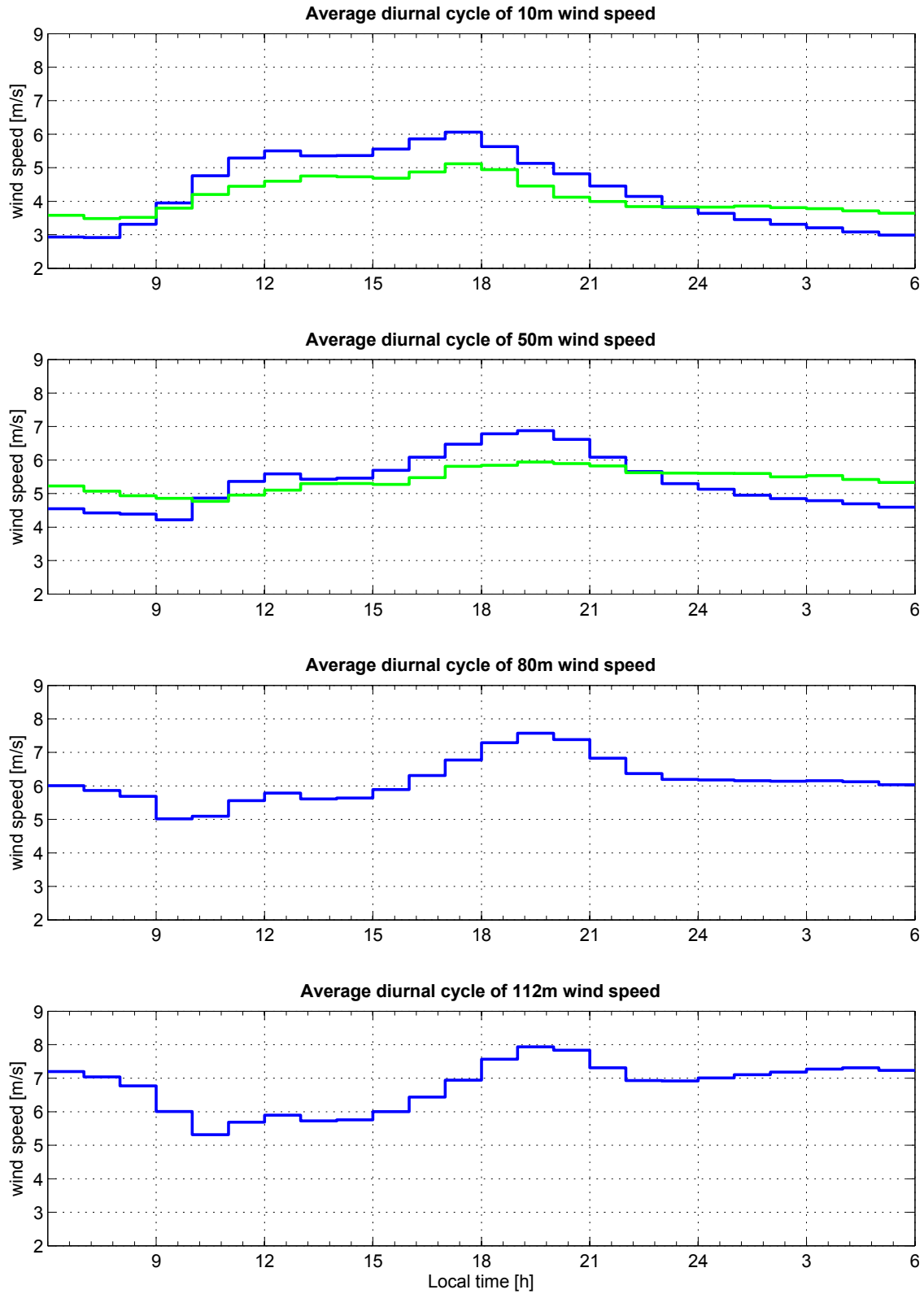


Figure 20: Average diurnal cycle of wind speeds at different heights as indicated in the panel titles for Jikiali. Simulated wind speeds are in blue, observed in green.

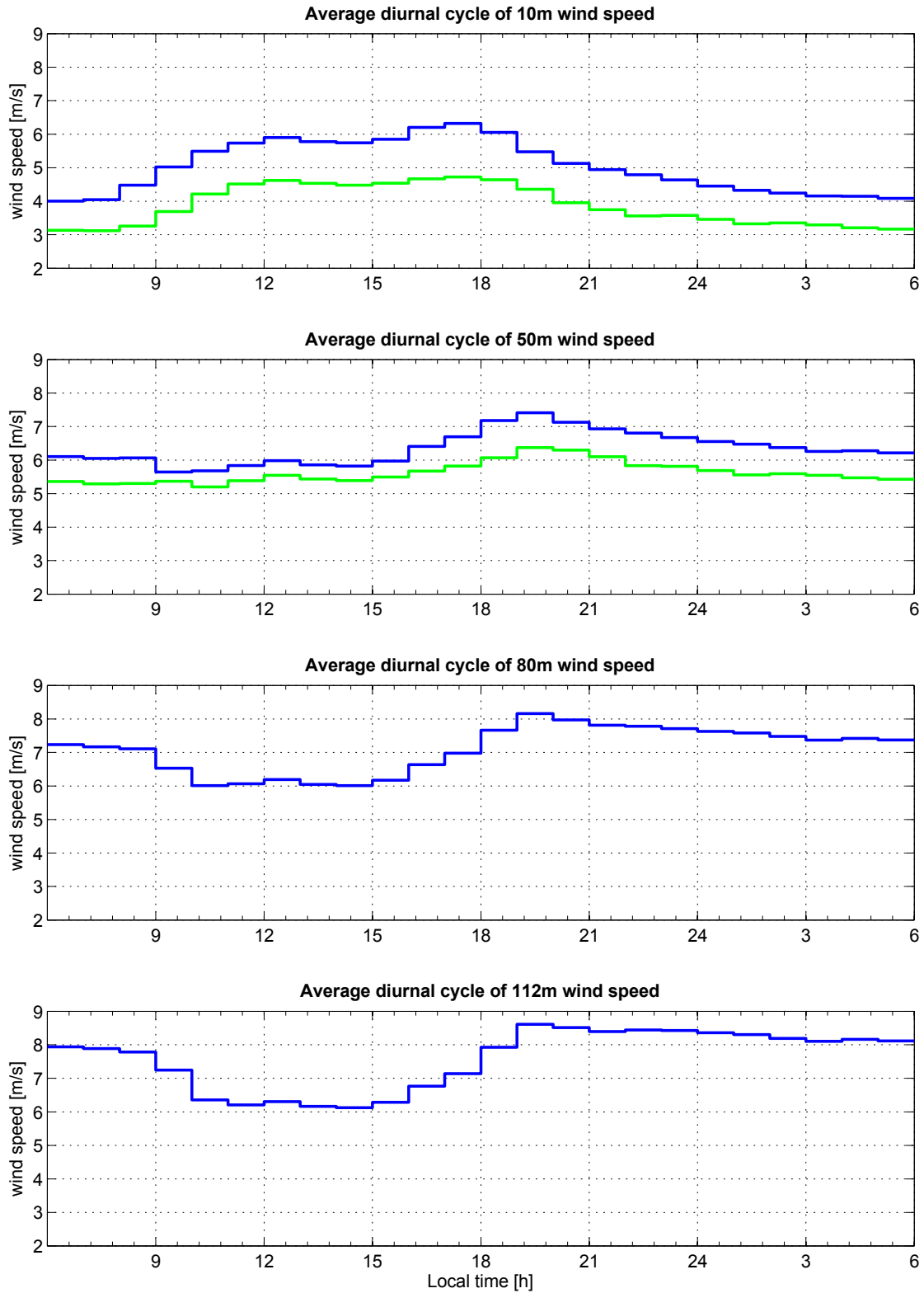


Figure 21: Average diurnal cycle of wind speeds at different heights as indicated in the panel titles for Balava. Simulated wind speeds are in blue, observed in green.

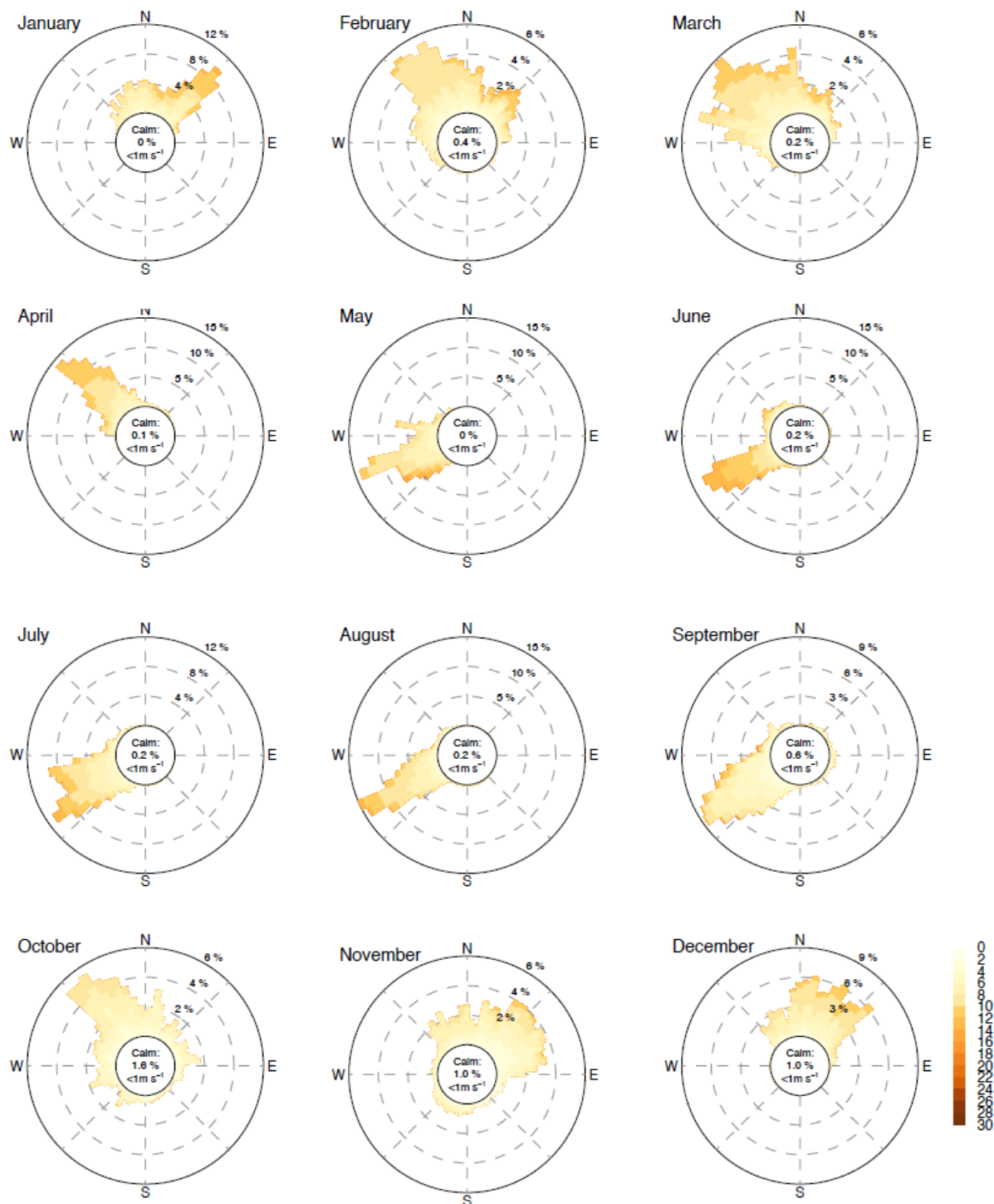


Figure 22: Wind roses for every month of the year 2011 as modeled by WRF for 80 m for Balava.

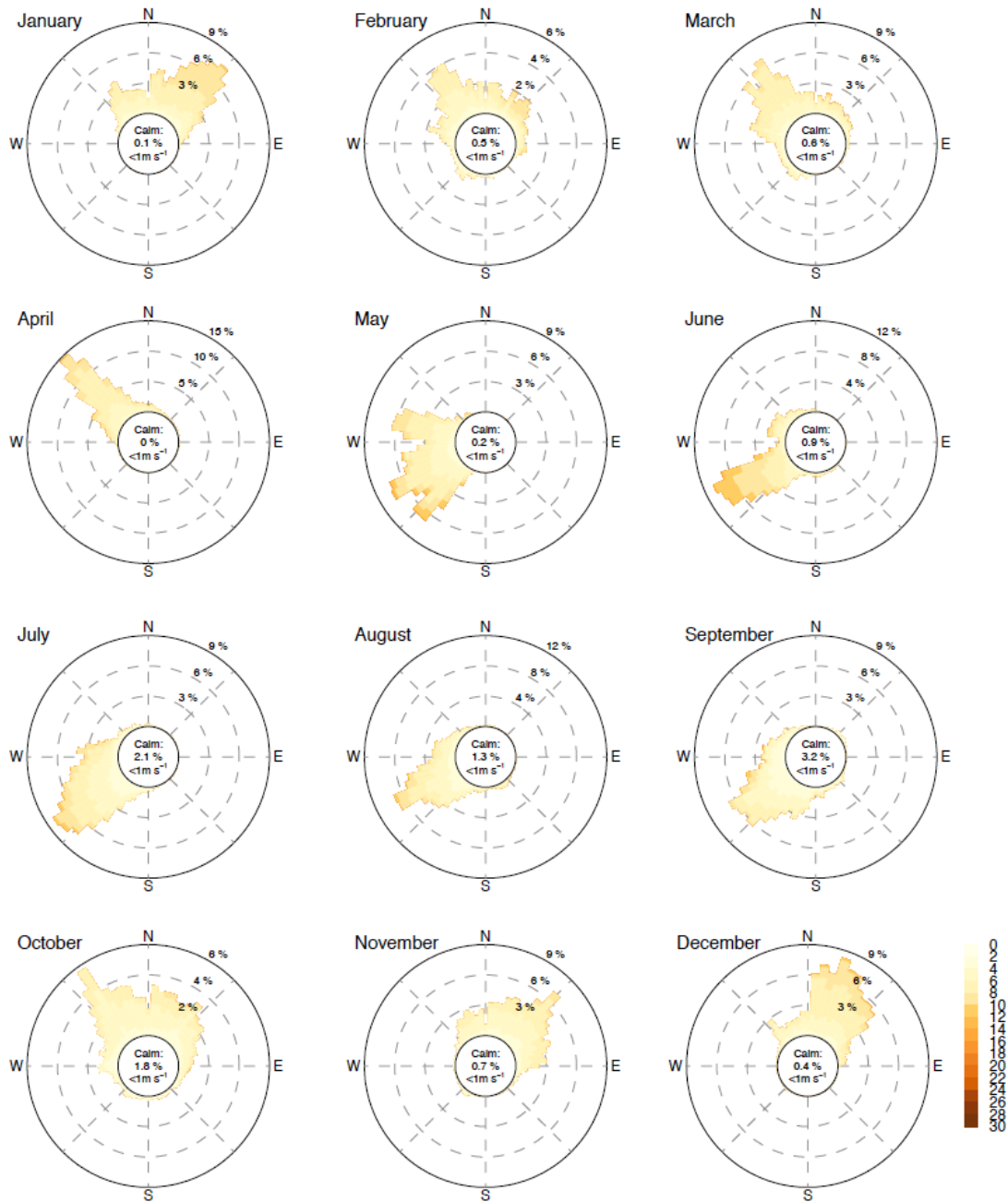


Figure 23: Wind roses of measured wind speed and direction for every month of the year 2011 for Balava.

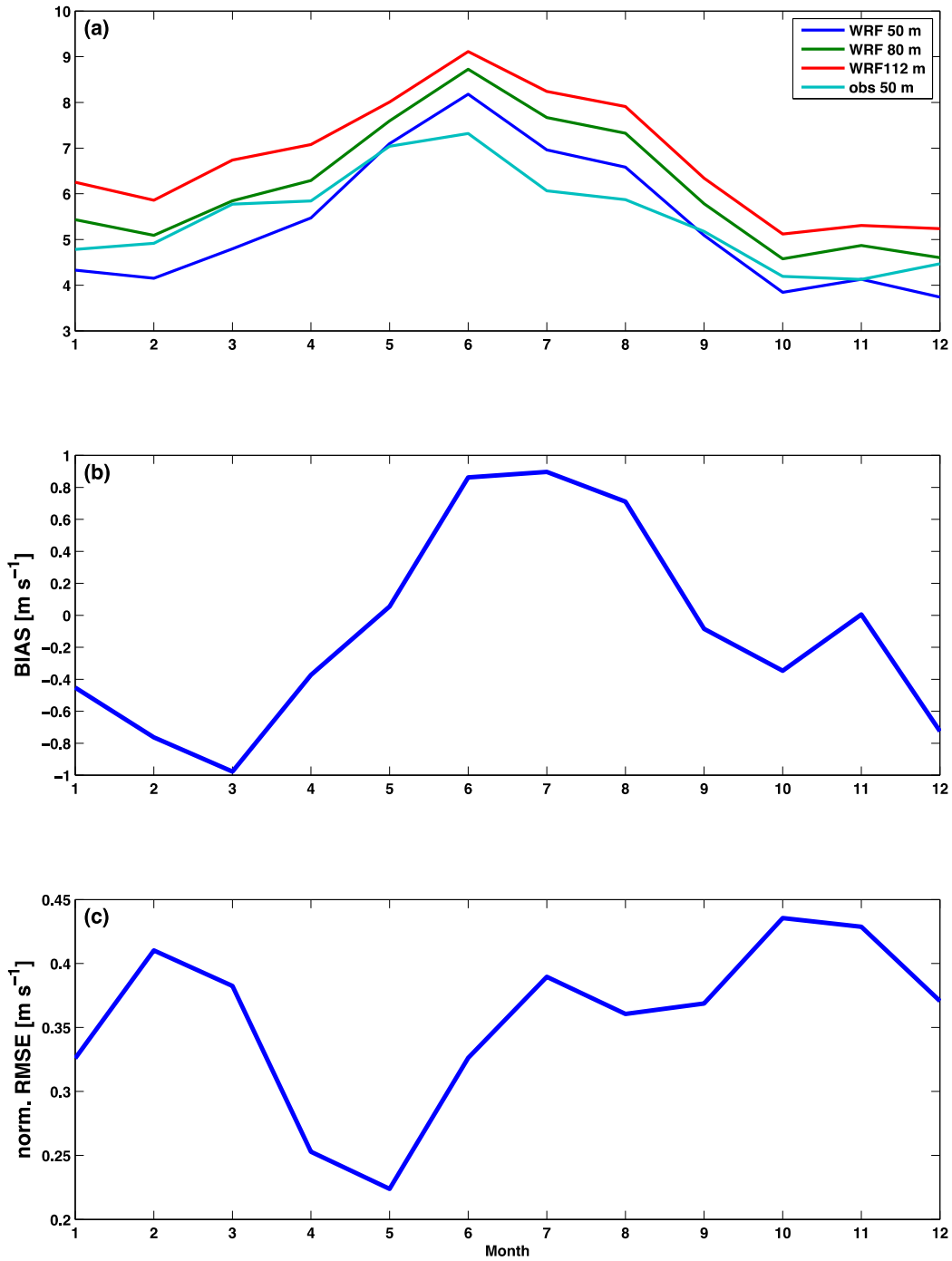


Figure 24: Annual cycle of simulated wind speed at 50 m, 80 m, and 112 m, and observed wind speeds at 50 m (panel a), wind speed bias for winds at 50 m (simulated minus observed; panel b), and normalized RMSE of wind speeds at 50 m (panel c) for Jikiali.

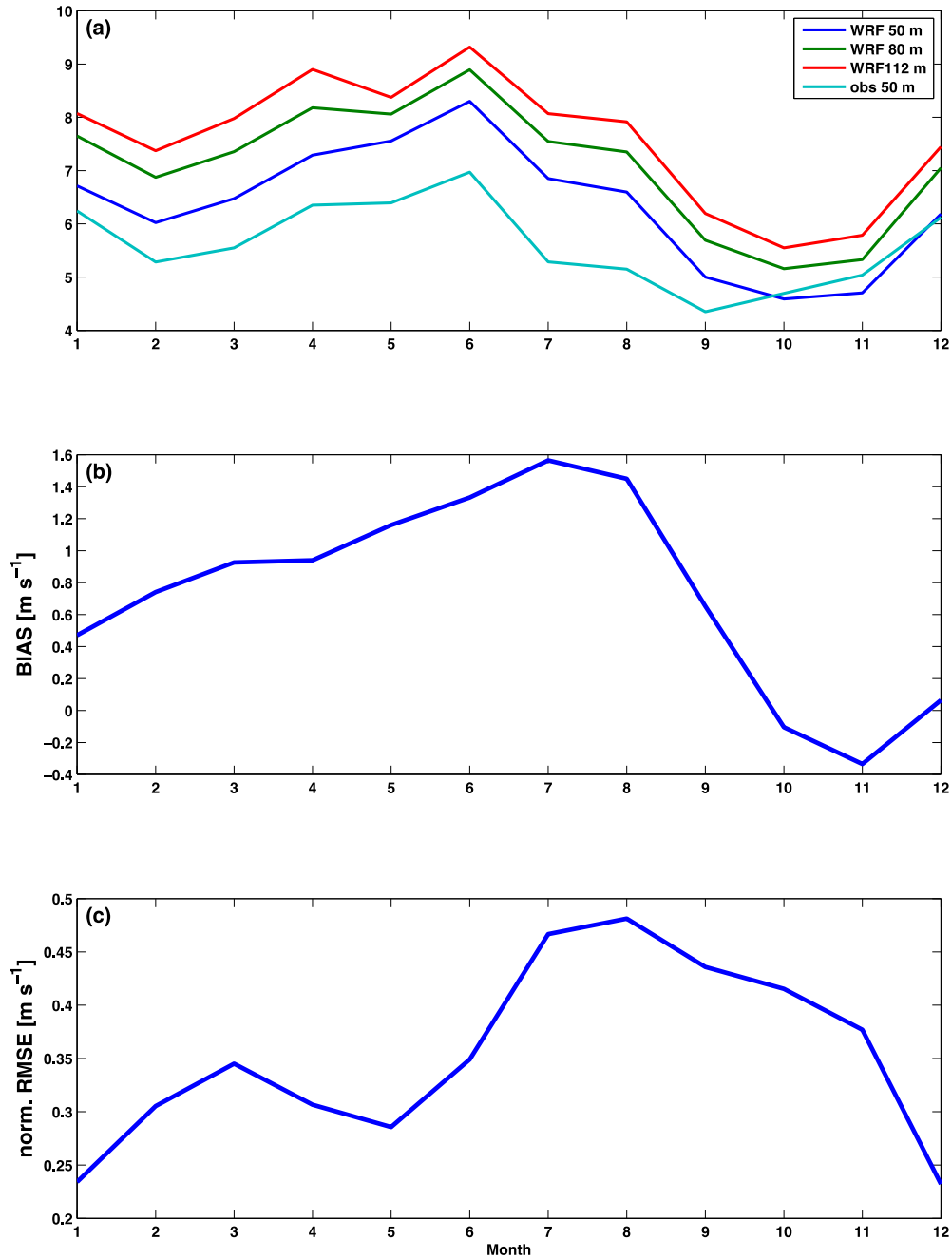


Figure 25: Annual cycle of simulated wind speed at 50 m, 80 m, and 112 m, and observed wind speeds at 50 m (panel a), wind speed bias for winds at 50 m (simulated minus observed; panel b), and normalized RMSE of wind speeds at 50 m (panel c) for Balava.

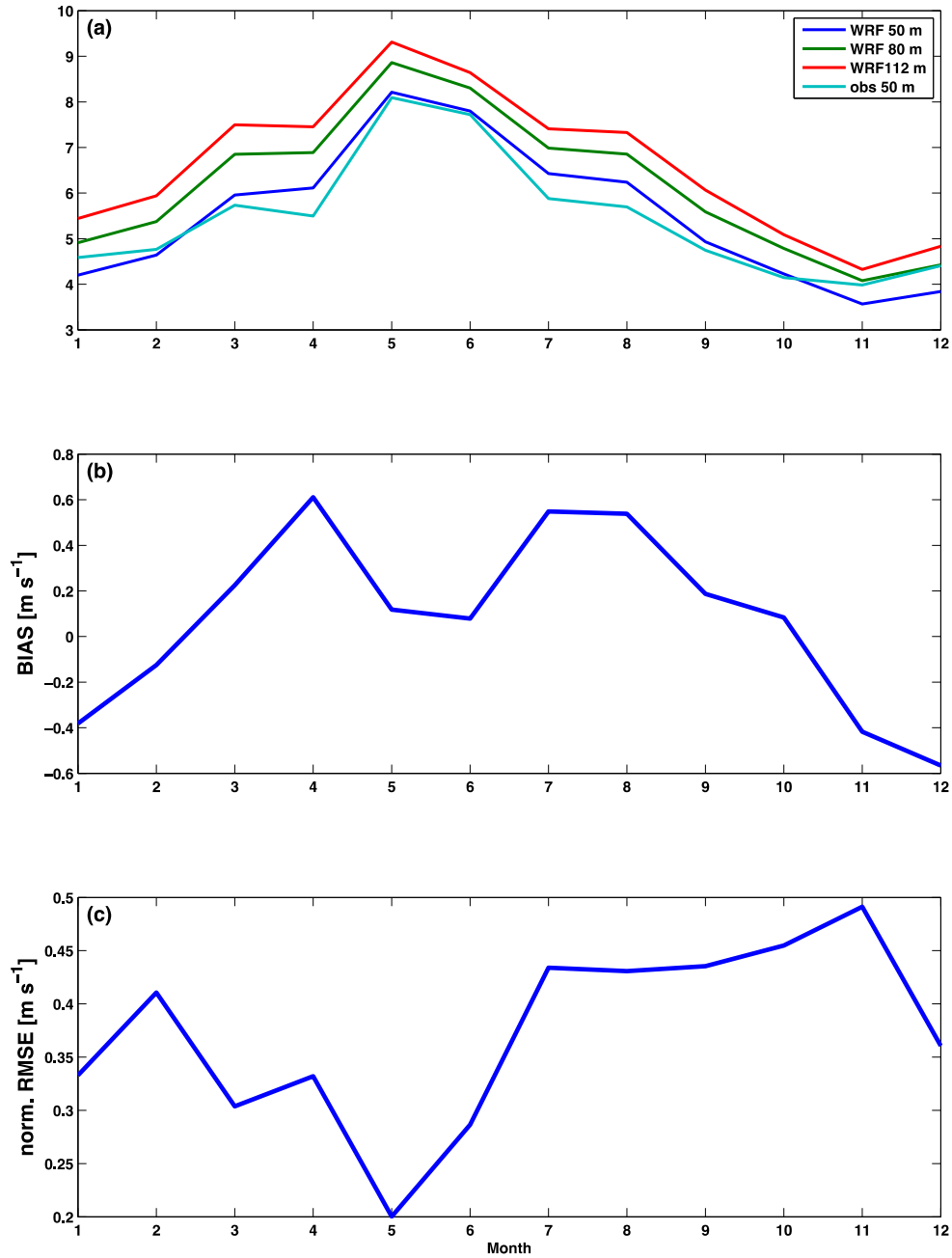


Figure 26: Annual cycle of simulated wind speed at 50 m, 80 m, and 112 m, and observed wind speeds at 50 m (panel a), wind speed bias for winds at 50 m (simulated minus observed; panel b), and normalized RMSE of wind speeds at 50 m (panel c) for Jegawa.

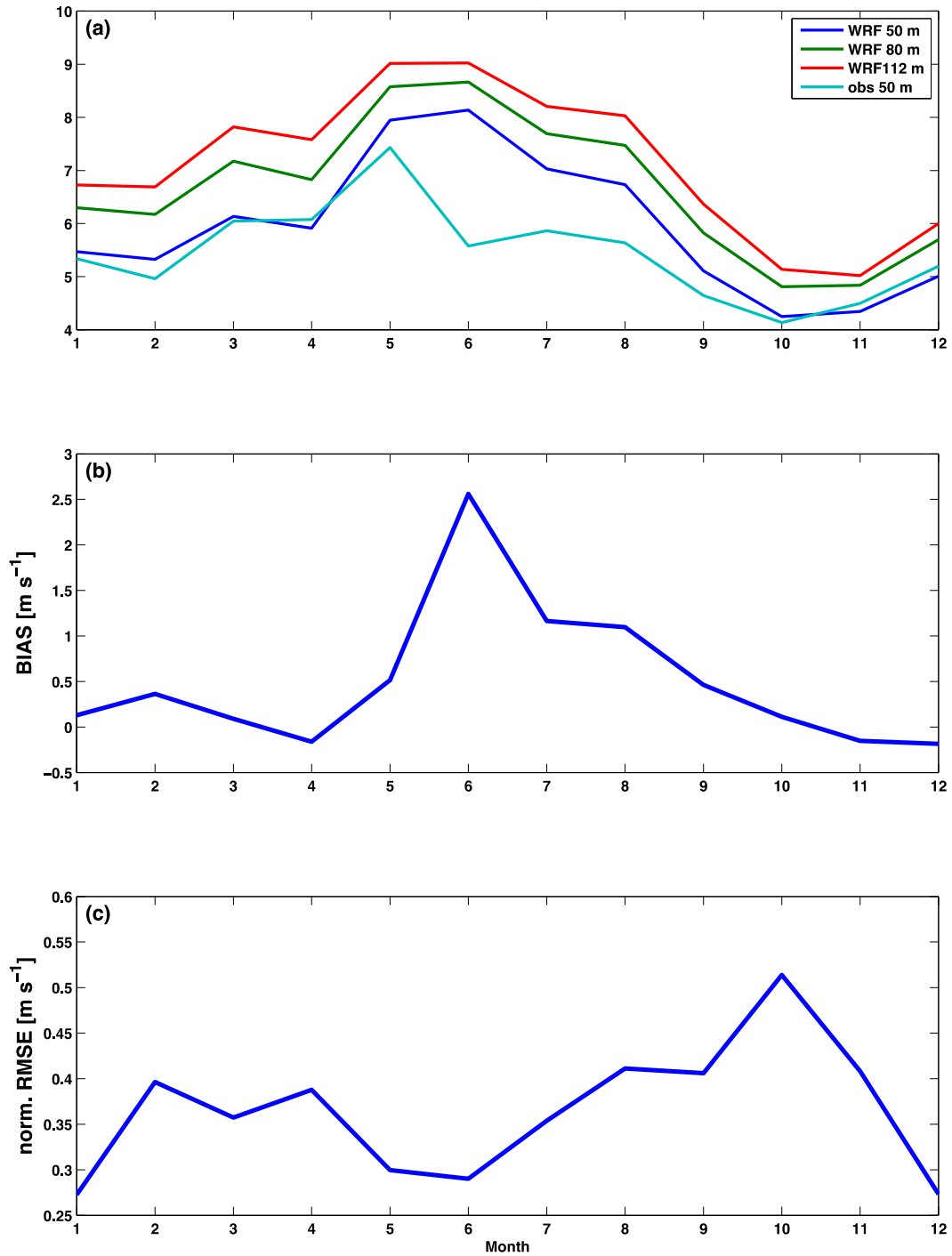


Figure 27: Annual cycle of simulated wind speed at 50 m, 80 m, and 112 m, and observed wind speeds at 50 m (panel a), wind speed bias for winds at 50 m (simulated minus observed; panel b), and normalized RMSE of wind speeds at 50 m (panel c) for Virewa.

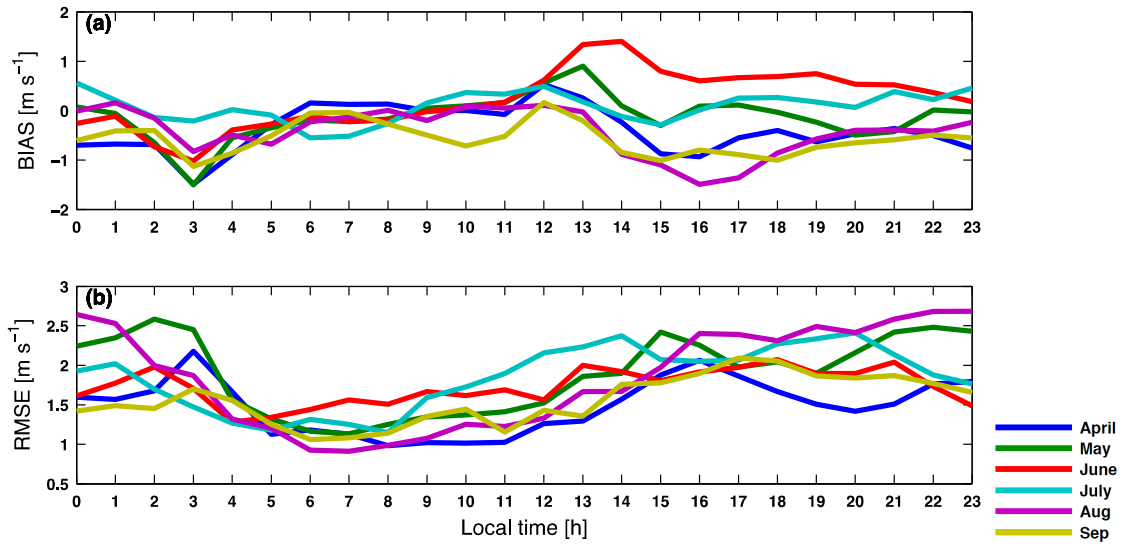


Figure 28: Diurnal cycle of (a) bias and (b) RMSE of wind speeds at 50 m for the winter months (January, February, March, October, November, December) for Jegawa.

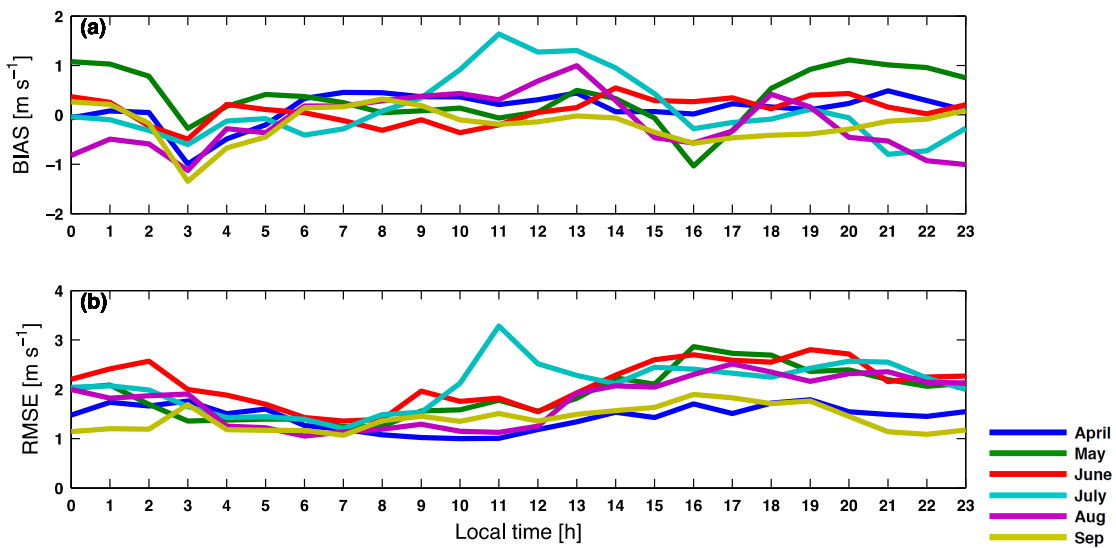


Figure 29: Diurnal cycle of (a) bias and (b) RMSE of wind speeds at 50 m for the winter months (January, February, March, October, November, December) for Virewa.

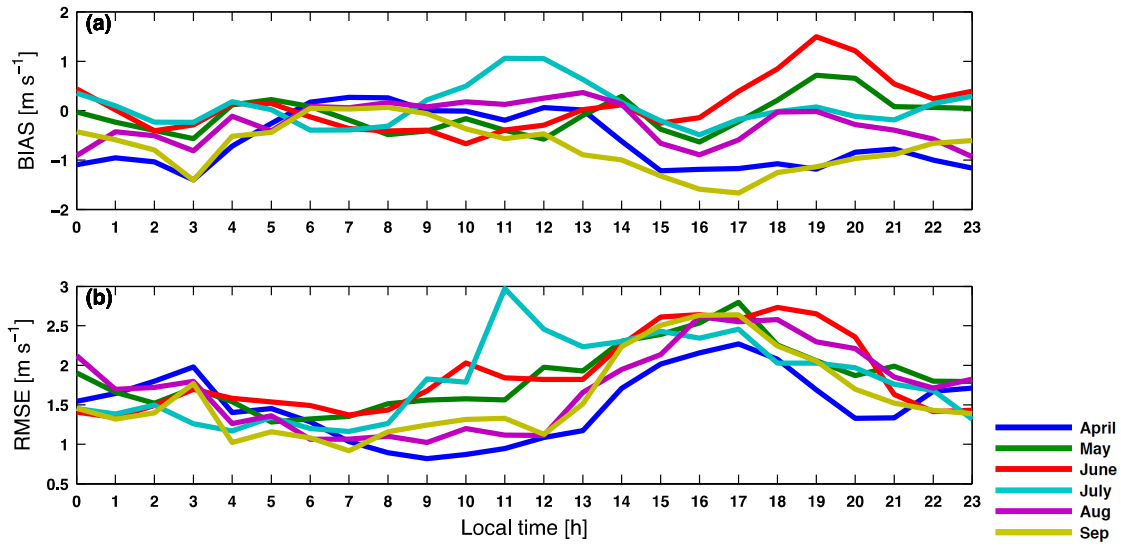


Figure 30: Diurnal cycle of (a) bias and (b) RMSE of wind speeds at 50 m for the winter months (January, February, March, October, November, December) for Sarva.

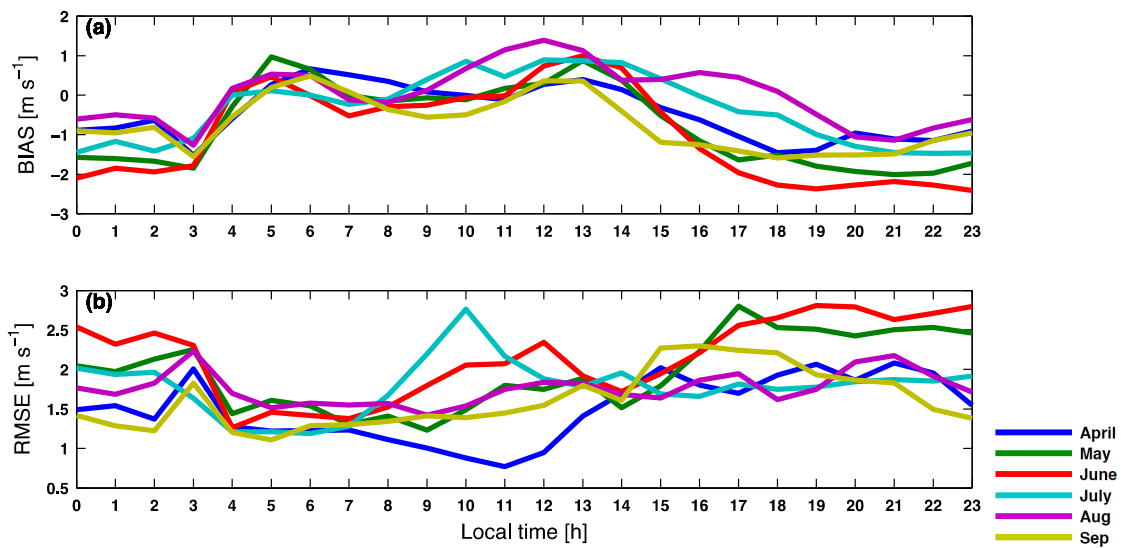


Figure 31: Diurnal cycle of (a) bias and (b) RMSE of wind speeds at 50 m for the winter months (January, February, March, October, November, December) for Jikiali.

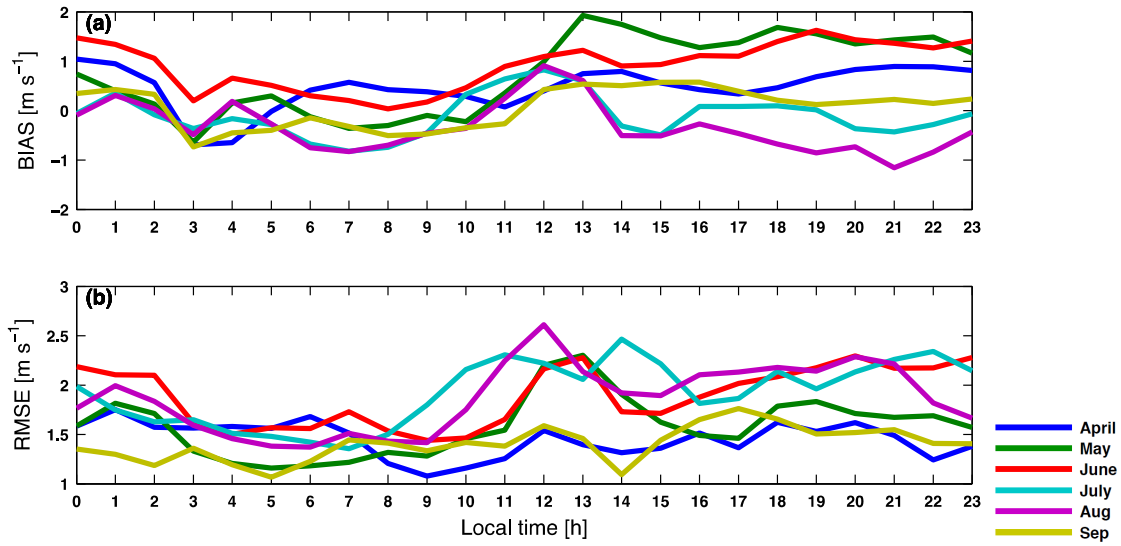


Figure 32: Diurnal cycle of (a) bias and (b) RMSE of wind speeds at 50 m for the winter months (January, February, March, October, November, December) for Balava.

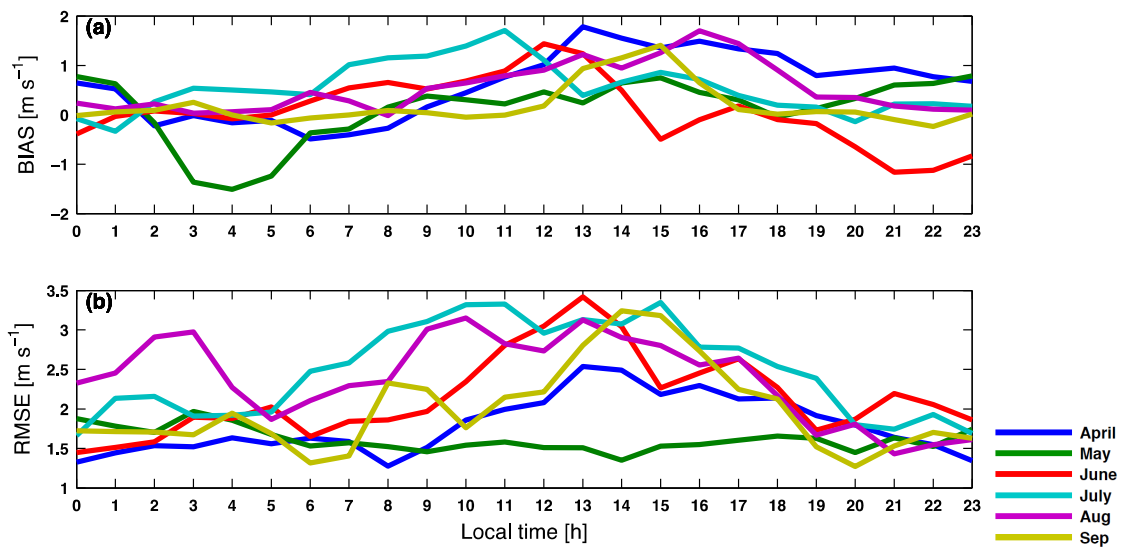


Figure 33: Diurnal cycle of (a) bias and (b) RMSE of wind speeds at 50 m for the summer months (April, May, June, July, August, September) for Jegawa.

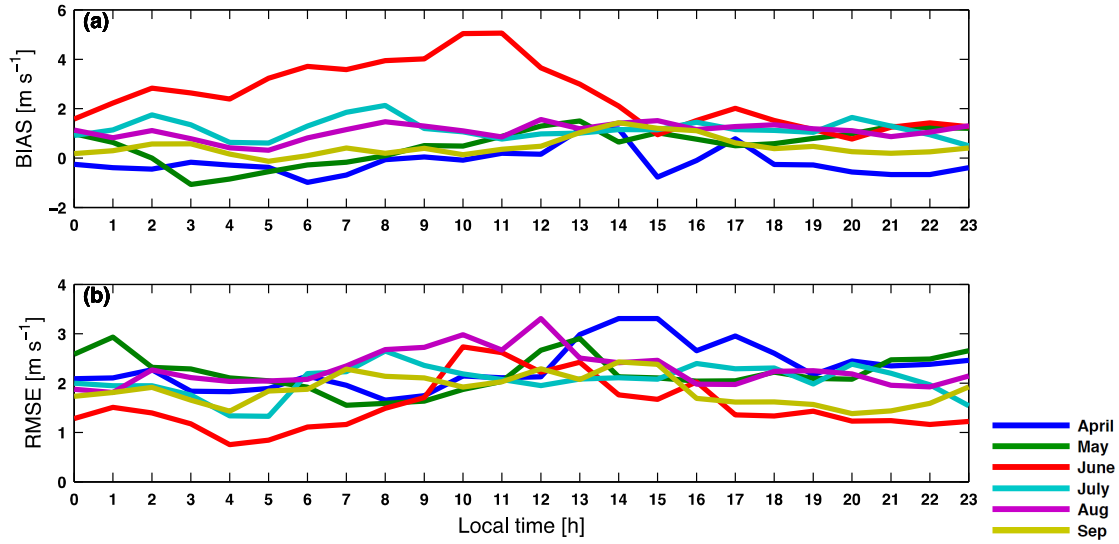


Figure 34: Diurnal cycle of (a) bias and (b) RMSE of wind speeds at 50 m for the summer months (April, May, June, July, August, September) for Virewa.

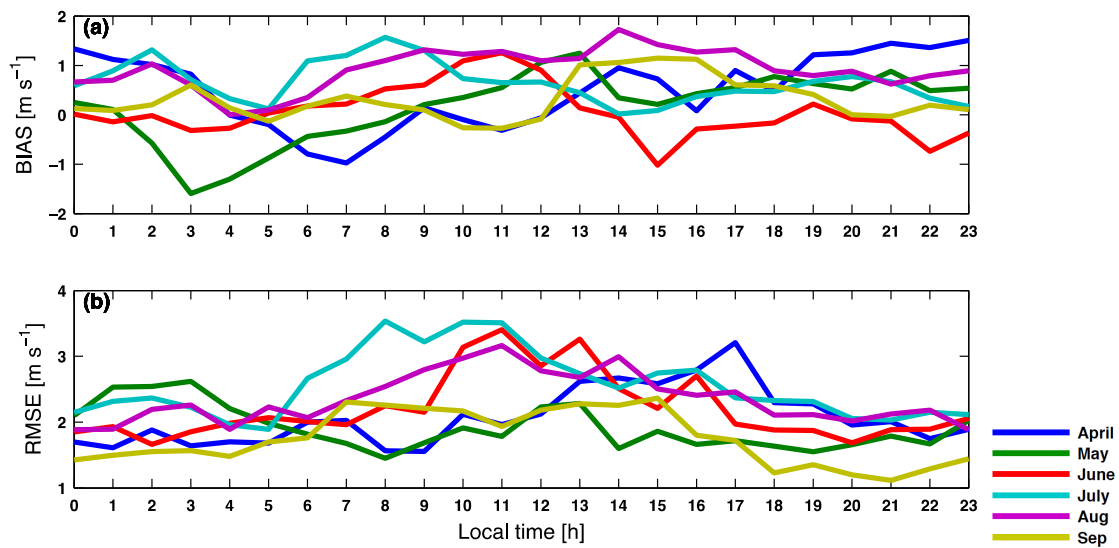


Figure 35: Diurnal cycle of (a) bias and (b) RMSE of wind speeds at 50 m for the summer months (April, May, June, July, August, September) for Sarva.

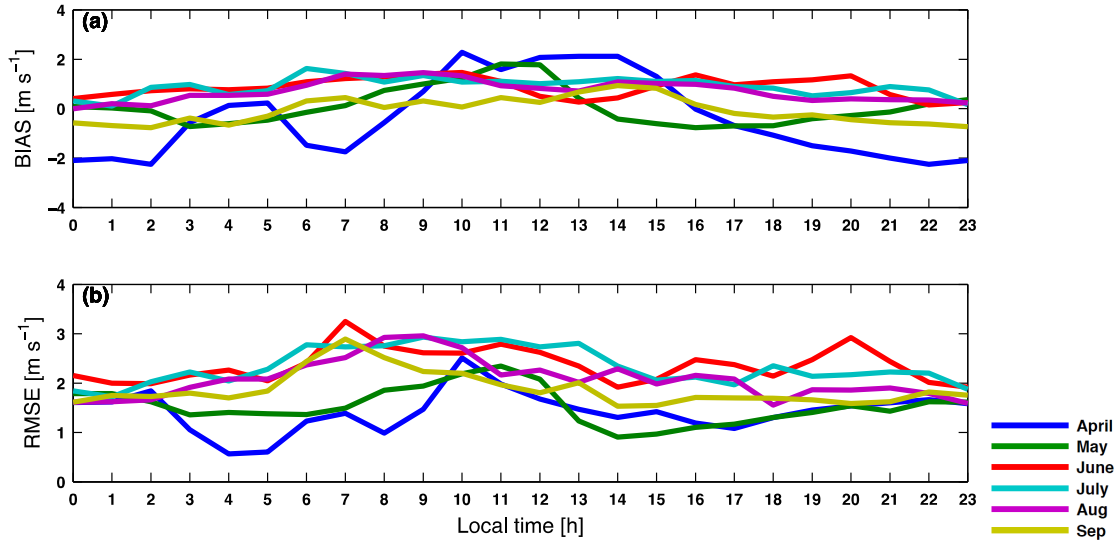


Figure 36: Diurnal cycle of (a) bias and (b) RMSE of wind speeds at 50 m for the summer months (April, May, June, July, August, September) for Jikiali.

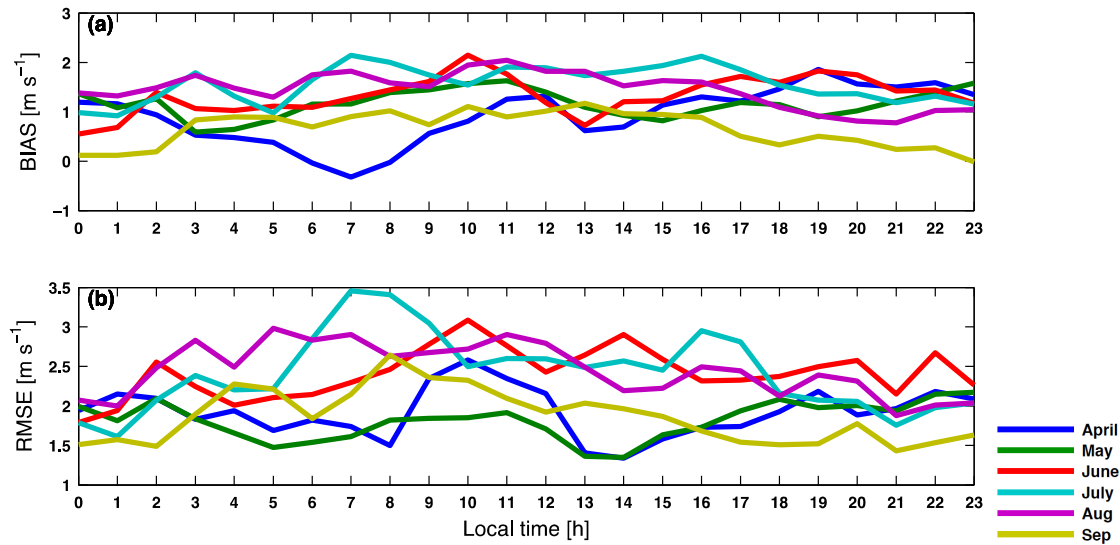


Figure 37: Diurnal cycle of (a) bias and (b) RMSE of wind speeds at 50 m for the summer months (April, May, June, July, August, September) for Balava.